# One-Step Synthesis of 1,3- and 1,1'-Diarylated Ferrocenes toward Main-Chain Metallomacrocycles

Wenjuan Li,*[a] Yuanping Li,[b] Yanting Shi,[b] Hui Xu,[b] Linyun Zhu,[b] Xinyu Chen,[b] Xiaopei Li,[a] Jianfeng Yan,[b] Lantao Liu,*[a] Yuanming Li*[b]

[a] *Henan Key Laboratory of Biomarker Detection and Diagnosis for Neurodegenerative Diseases, Shangqiu Normal University, Shangqiu, 476000, China. E-mail: liult05@iccas.ac.cn (L. Liu), liwj0523@126.com (W. Li)*

[b] *Key Laboratory of Advanced Carbon-Based Functional Materials (Fujian Province University), College of Chemistry, Fuzhou University, Fuzhou, 350108, China. E-mail: yuanming.li@fzu.edu.cn (Y. Li).*

[+] *These authors contributed equally to this work.*

# Table of contents

## 1. General Information

### 1) Reagent

Reagents were purchased from commercial sources and used directly without further purification unless mentioned otherwise. Unless otherwise noted, all reactions were carried out under an argon atmosphere using anhydrous, deoxygenated, and ultra-dry solvents via standard Schlenk techniques. The special anhydrous solvent treatment as follows:

Redistillation of toluene: Toluene was refluxed over sodium metal for 4-5 hours. The toluene collected in the condenser was then transferred to and stored in a bottle containing activated molecular sieves.

### 2) Characterization

$^{1}H$ and $^{13}C$ NMR spectra were recorded at 298 K on a JNM-ECZ600R instrument. The residual deuterated solvent signal was used as the internal reference in NMR spectra ($CDCl_3$ δ [ppm] = 7.26 for $^{1}H$ NMR, δ [ppm] =77.16 for $^{13}C$ NMR). High-resolution mass spectra (HRMS) were acquired on the Thermo Scientific Exactive Plus Mass spectrometer equipped with an electrospray ionization (ESI) source. Single-crystal X-ray data were collected at 100 K on a Synergy Custom (Liquid MetalJet D2+) diffractometer equipped with Ga-Kα ($\lambda$ = 1.34050) and reduction was performed by using the program CrysAlisPro, [1] [1] [1] [1] and collected at 298 K on a Rigaku-AFC7 equipped with a Rigaku Saturn CCD area-detector system using monochromatic Mo Kα radiation ($\lambda$ = 0.71073 Å). The structures were solved by the direct method and refined by full-matrix least-squares on $F^2$ using SHELXTL and OLEX2.[2, 3] The UV-Vis spectra were recorded on a UV-2700 spectrometer. The CV curves were recorded on Matrohm Autolab and CHI 760E potentiostat (Chinstruments) at room temperature, working electrode: glassy carbon (3 mm-diameter circular base with a geometric surface area of 0.071 $cm^2$); counter electrode: Pt; reference electrode: Ag/AgCl (3.0 mol/L KCl solution), scan ratio: 100 mV/s, concentration: 0.1 mM in DCM. The measurements were carried out in $Bu_4NPF_6$ (0.1 M) as a supporting electrolyte. Prior to use, it was polished with alumina ($Al_2O_3$) suspension to reduce surface roughness.

## 2. General procedure of synthesis of disubstituted ferrocene

**Synthesis of 4-chlorophenyl-substituted ferrocene**

Preparation of the ferrocenium salt: Ferrocene (465 mg, 2.5 mmol, 1.0 eq.) and concentrated sulfuric acid (3 mL) were added to a 30 mL test tube. The mixture was stirred at room temperature for 2 h. After completion, the reaction mixture was poured into a 100 mL round-bottom flask containing 12.5 g of crushed ice and allowed to warm to room temperature.

Preparation of the aryl diazonium salt: 4-chloroaniline (829 mg, 6.5 mmol, 2.6 eq.) was dissolved in a mixture of water/concentrated HCl (5.4 mL, v/v = 1/1) to form Solution A, and then was placed in an ice-water bath. The $NaNO_2$ (483 mg, 7.0 mmol, 2.8 eq.) was dissolved in water (2.7 mL) to form Solution B, which was also placed in an ice-water bath. Solution B was added dropwise to Solution A via a pipette. After the addition was complete, the mixture was stirred in the ice-water bath for an additional 30 min.

Copper powder (250 mg, 4.0 mmol, 1.6 eq.) was added to the ferrocenium salt solution. The freshly prepared aryl diazonium salt solution was then added dropwise to this mixture. After the addition, the reaction was allowed to proceed in a pre-heated oil bath at 45 °C for 24 h. Upon completion, ascorbic acid (625 mg) was added, and stirring was continued for 1 h. The mixture was then extracted with dichloromethane (3 × 15 mL). The combined organic extracts were filtered through a Celite pad, and the solvent was removed under reduced pressure to afford the crude product. The crude product was purified by column chromatography on 200-300 mesh silica gel (eluent: Petroleum Ether) to give a mixture of the 1,3-disubstituted and 1,1'-disubstituted regioisomers. Further purification by column chromatography on 300-400 mesh silica gel (eluent: Petroleum Ether) yielded the pure 1,3-disubstituted product and 1,1'-disubstituted products.

**1,3-FcCl**: red solid (71 mg), isolated yield: 7%. $^1$H NMR (600 MHz, $CDCl_3$) δ: 7.44 (d, J = 8.1 Hz, 4H), 7.28 (d, J = 8.0 Hz, 4H), 5.09 (s, 1H), 4.79 (s, 2H), 3.93 (s, 5H). $^{13}$C NMR (151 MHz, $CDCl_3$) δ: 137.5, 131.9, 128.7, 127.3, 85.4, 71.5, 67.6, 65.0. HRMS (ESI): m/z calculated for $C_{22}H_{16}Cl_2Fe$ $[M]^+$: 405.9978, found: 405.9921.

**1,1'-FcCl:** red solid (244 mg), isolated yield: 24% $^1$H NMR (600 MHz, Chloroform-*d*) δ 7.13 (s, 8H), 4.45 (t, *J* = 1.8 Hz, 4H), 4.25 (t, *J* = 1.8 Hz, 4H), which is consistent with literature reports.[4]

**1,2-FcCl**: Column chromatography separation was attempted using 300–400 mesh silica gel with

an eluent gradient from petroleum ether: dichloromethane (5:0) to (5:1). After repeated column runs, a mixture containing minor amounts of 1-FcCl and 1,3-FcCl along with other by-products (liquid) were obtained. Further crystallization did not yield any pure 1,2-FcCl. In addition, attempts were made to purify the target compound by thin-layer chromatography and Gel Permeation Chromatography, but none of these methods afforded the pure compound.

**Synthesis of 4-bromophenyl-substituted ferrocene**

4-bromophenyl-substituted ferrocene was prepared according to the general procedure with 4-bromoaniline (1.121 g, 6.5 mmol, 2.6 eq.) and purified by silica gel column chromatography (petroleum ether), giving products as red solids.

**1,3-FcBr**: red solid (50 mg), isolated yield: 4%. $^{1}$H NMR (600 MHz, $CDCl_3$) δ: 7.45 - 7.41 (m, 4H), 7.38 (d, J = 8.6 Hz, 4H), 5.09 (s, 1H), 4.79 (s, 2H), 3.92 (s, 5H). $^{13}$C NMR (151 MHz, $CDCl_3$) δ: 138.1, 131.7, 127.7, 119.9, 85.4, 71.6, 67.6, 65.0. HRMS (ESI): m/z calculated for $C_{22}H_{16}Br_2Fe$ $[M]^+$: 493.8968, found: 493.8959.

**1,1'-FcBr**: red solid (248 mg), isolated yield: 20%. $^{1}$H NMR (600 MHz, Chloroform-*d*) δ 7.28 – 7.26 (m, 4H), 7.08 – 7.05 (m, 4H), 4.45 (t, *J* = 1.9 Hz, 4H), 4.25 – 4.23 (m, 4H), which is consistent with literature reports.[5]

**1-FcBr**: red solid (35 mg), isolated yield: 4%. $^{1}$H NMR (600 MHz, Chloroform-*d*) δ 7.41 – 7.38 (m, 2H), 7.34 – 7.31 (m, 2H), 4.63 (s, 2H), 4.35 (s, 2H), 4.05 (s, 5H), which is consistent with literature reports.[6]

**Synthesis of 4-bromophenyl-substituted ferrocene (Using TEMPO as a Radical Trapping Agent)**

Using 4-bromoaniline (1.121 g, 6.5 mmol, 2.6 equivalents) as the starting material, 4-bromophenyl-substituted ferrocene was prepared following the standard procedure (after adding copper powder, two equivalents of TEMPO were subsequently added, with subsequent steps identical to above). Purification via silica gel column chromatography (petroleum ether) yielded a red solid. (Crude NMR yields: 1-FcBr, 11%; 1,1'-FcBr, 2.1%; 1,3-FcBr, 0.5%; 1,2-FcBr, 0.5%)

**Synthesis of 4-fluorophenyl-substituted ferrocene**

4-fluorophenyl-substituted ferrocenes were prepared according to the general procedure with 4-fluoroaniline (721 mg, 6.5 mmol, 2.6 eq.) and purified by silica gel column chromatography (petroleum ether), giving products as red solids.

**1,1'-FcF**: red solid (65 mg), isolated yield: 4.4% $^1$H NMR (600 MHz, Chloroform-d) δ 7.22 – 7.17 (m, 4H), 6.90 – 6.85 (m, 4H), 4.42 (t, J = 1.9 Hz, 4H), 4.22 (t, J = 1.8 Hz, 4H), which is consistent with literature reports.[7]

**1-FcF**: red solid (58 mg), isolated yield: 6%.$^1$H NMR (600 MHz, Chloroform-*d*) δ 7.45 – 7.41 (m, 2H), 7.01 – 6.96 (m, 2H), 4.59 (t, *J* = 1.8 Hz, 2H), 4.31 (t, *J* = 1.8 Hz, 2H), 4.05 (s, 5H), which is consistent with literature reports.[8]

**Synthesis of 4-nitrophenyl-substituted ferrocene**

4-nitrophenyl-substituted ferrocenes were prepared according to the general procedure with 4-nitroaniline (898 mg, 6.5 mmol, 2.6 eq.) and purified by silica gel column chromatography (petroleum ether), giving products as red solids.

**1-FcNO$_2$**: red solid (31 mg), isolated yield: 4%.$^1$H NMR (600 MHz, Chloroform-*d*) δ 7.45 – 7.41 (m, 2H), 7.01 – 6.96 (m, 2H), 4.59 (t, *J* = 1.8 Hz, 2H), 4.31 (t, *J* = 1.8 Hz, 2H), 4.05 (s, 5H), which is consistent with literature reports. [9] [8] [9] [9] [9]

## 3. Optimization of Reaction Conditions

The reaction temperature was first investigated using 4-chlorobenzenediazonium chloride as the model substrate. The total yield of disubstituted ferrocene derivatives (**1,1'-FcCl**, **1,3-FcCl**, and **1,2-FcCl**) first increased and then decreased, reaching a maximum of 46% at 40°C, at which point the yields of 1,1'-bis(4-chlorophenyl)ferrocene (**1,1'-FcCl**, 24%) and 1,3-bis(4-chlorophenyl)ferrocene (**1,3-FcCl**, 7%) reached its maximum, while the proportion of monosubstituted products fell to its lowest. Subsequent optimization of the diazonium salt amount revealed that 2.6 equivalents relative to ferrocene afforded the highest yields of **1,1'-FcCl** (25%) and **1,3-FcCl** (8%). Furthermore, the copper powder (1.6 equiv.) proved superior to all tested cuprous salts, delivering the maximal yields of **1,1'-FcCl** (25%) and **1,3-FcCl** (8%).

**Table S1.** The effects of temperature and diazonium salt concentration on the reaction

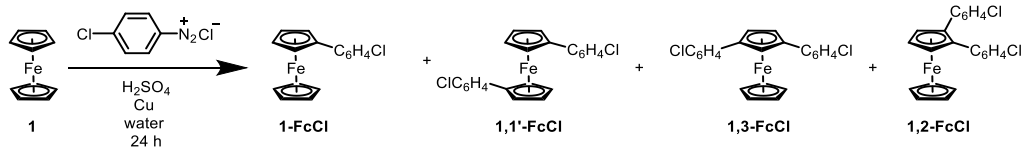


| Entry | T (°C) | Azo (eq) | Substrate | Products | | | | Total yield of disubstituted ferrocene |
|---|---|---|---|---|---|---|---|---|
| | | | **1** | **1-FcCl** | **1,1'-FcCl** | **1,3-FcCl** | **1,2-FcCl** | **(1,1'-FcCl + 1,3-FcCl + 1,2-FcCl)** |
| 1 | 25 | 1 | 2% | 13% | 15% | 4% | 8% | 27% |
| 2 | 30 | 1 | 1% | 10% | 18% | 5% | 10% | 33% |
| 3 | 35 | 1 | 4% | 7% | 23% | 7% | 12% | 42% |
| 4 | 40 | 1 | 0.8% | 5% | 24% | 7% | 14% | 45% |
| 5 | 45 | 1 | 3% | 9% | 23% | 7% | 12% | 42% |
| 6 | 50 | 1 | 0.7% | 7% | 22% | 7% | 12% | 41% |
| 7 | 40 | 2.0 | 5% | 10% | 18% | 6% | 9% | 33% |
| 8 | 40 | 2.2 | 2% | 9% | 21% | 6% | 11% | 38% |
| 9 | 40 | 2.4 | 3% | 9% | 23% | 7% | 12% | 42% |
| 10 | 40 | 2.6 | 0.8% | 8% | 25% | 8% | 13% | 46% |
| 11 | 40 | 2.8 | 0.3% | 4% | 17% | 5% | 9% | 31% |
| 12 | 40 | 3.0 | 0.3% | 5% | 17% | 5% | 9% | 31% |
| 13 | 40 | 3.2 | 0.2% | 5% | 19% | 6% | 11% | 36% |

**Table S2.** Effect of additive

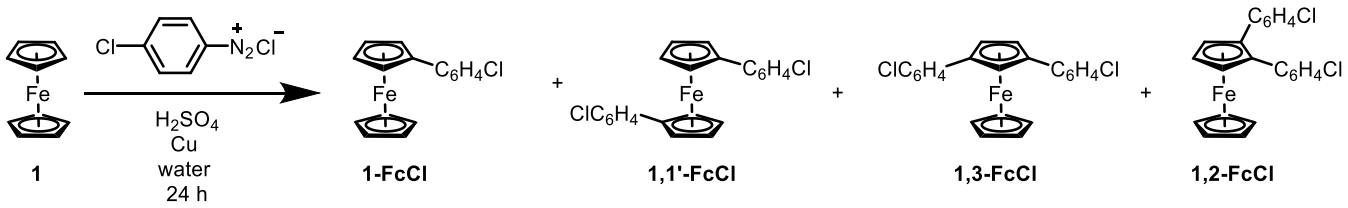


| entry | Additive (eq.) | Substrate | Products | | | | Total yield of disubstituted ferrocene (1,1'-FcCl + 1,3-FcCl + 1,2-FcCl) |
|---|---|---|---|---|---|---|---|
| | | 1 | 1-FcCl | 1,1'-FcCl | 1,3-FcCl | 1,2-FcCl | |
| 1 | - | 1% | 8% | 18% | 5% | 8% | 31% |
| 2 | Cu (1.6) | 0.8% | 8% | 25% | 8% | 13% | 46% |
| 3 | Cu (3.2) | 0.5% | 4% | 18% | 5% | 9% | 32% |
| 4 | CuI (1.6) | 0.4% | 8% | 24% | 7% | 13% | 44% |
| 5 | CuBr (1.6) | 4% | 26% | 20% | 5% | 10% | 35% |
| 6 | CuCl (1.6) | 6% | 21% | 24% | 6% | 11% | 41% |

**Table S3.** The scope of differently substituted diazonium salts

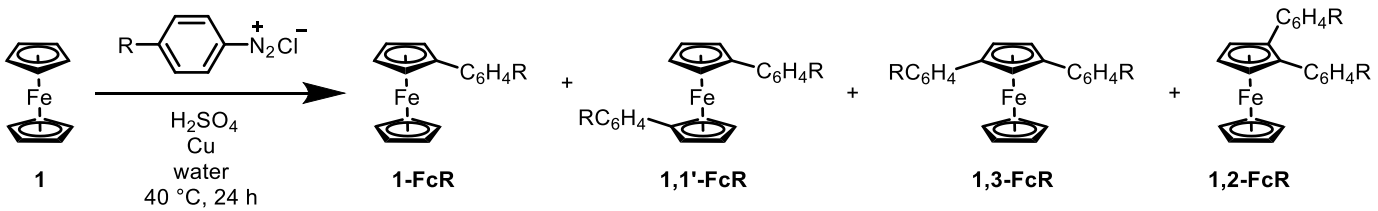


| Entry | R | Substrate | Products* | | | | Total yield of disubstituted ferrocene (**1,1'-FcR + 1,3-FcR + 1,2-FcR**) |
|---|---|---|---|---|---|---|---|
| | | **1** | **1-FcR** | **1,1'-FcR** | **1,3-FcR** | **1,2-FcR** | |
| 1 | Br | n.d. | 8% | 25% (20%) | 6%(4%) | 12% | 43% |
| 2 | Cl | n.d. | 9% | 26% (24%) | 8% (7%) | 15% | 49% |
| 3 | F | 2% (2%) | 8% (6%) | 11% | 3% | 13% (7%) | 26% |
| 4 | $NO_2$ | 2% (2%) | 6% (4%) | 3% | 2% | 2% (1%) | 7% |
| 5 | MeO | 4% | 3% | 13% | 2% | 10% | 25% |
| 7 | H | 21% (21%) | 27% (26%) | 6% | 2% | 6% | 14% |

*Yield was determined by $^1$H NMR spectroscopy, and the separation yield is shown in parentheses.

## 4. Gram Experiment

To explore the practicality of the reaction, a gram-scale preparation of the chloroaryl-substituted product was conducted. The reaction was scaled up to 40 mmol under the standard conditions, and the final product yield was consistent with the small-scale results. Ultimately, 2.87 g of the 1,1'-disubstituted product and 610 mg of the 1,3-disubstituted product were isolated.

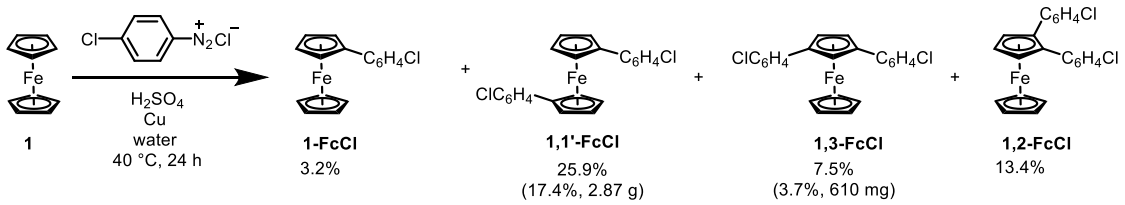


## 5. Proposal Mechanism

Based on the above experimental results and previous report, [10] [9] [10] [10] [10] we propose the following reaction mechanism. Firstly, ferrocene is oxidized to ferrocene cation under the action of concentrated sulfuric acid, and then the aryl diazonium salt is reduced to aryl radical by copper. Aromatic radicals attack ferrocene cations to form complexes, where Csp3-H interacts with electron-deficient Fe atoms to deprotonate and form arylation products.

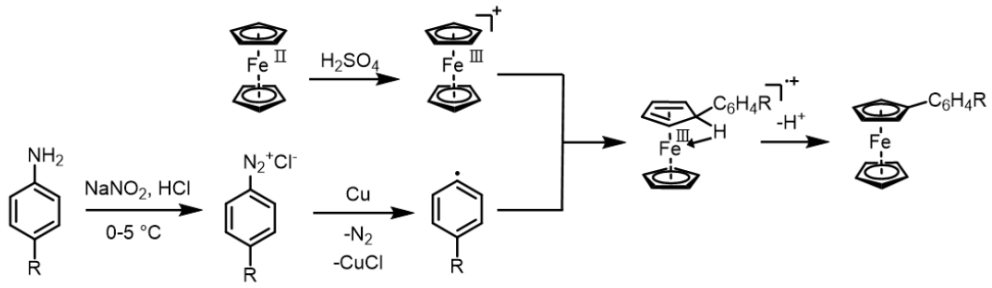


**Figure S1.** Proposal mechanism of the synthesis of arylated ferrocenes.

## 6. Synthesis of main-Fc[11]CPP

CsF (365 mg, 2.4 mmol, 24.0 eq.) was placeed in a 250 mL Schlenk reaction tube and dried in a bottle to remove water. Then **1,1'-FcBpin**[11] (59 mg, 0.1 mmol, 1.0 eq.) and 4,4"-bis(4,4,5,5-tetramethyl-1,3,2-dioxaborolan-2-yl)-1,1':4',1"-terphenyl[12] (169 mg, 0.35 mmol, 3.5 eq.) were added in turn. Subsequently, 80 mL of anhydrous dichloroethane (DCE) was added under a nitrogen atmosphere. The system was purged with nitrogen and evacuated three times using standard Schlenk techniques to ensure an inert environment. The reaction was conducted at a high dilution (concentration: 1.25 mM), a condition specifically designed to favor the cyclization process. Finally, the catalyst $Pt(cod)Cl_2$ (168 mg, 0.45 mmol, 4.5 eq.) was added and the mixture was stirred at room temperature for 30 minutes and then heated at 85℃ in an oil bath for 48 hours. After the reaction, the reaction bottle was cooled to room temperature, the solvent was removed by rotary evaporator, and the solvent was dried under vacuum. After adding methanol (75 mL), ultrasonic filtration, and washing with a small amount of methanol until the filtrate was colorless, the precipitate was collected and dried under vacuum.

The dried residue was transferred to a 100 mL Schlenk flask, and triphenylphosphine (1.06 g, 4.0 mmol, 40.0 eq.) was added. Finally, 32 mL of redistilled toluene was added, and the gas was exchanged three times using standard Schlenk techniques. Then the mixture was stirred at room temperature for 30 minutes, and then heated at 110℃ in an oil bath for 48 hours. After the reaction was completed, the reaction bottle was returned to room temperature, and the solvent was removed by rotary evaporator. The mixture was separated by silica gel column chromatography (dichloromethane/petroleum ether = 1/3-1/1). The **main-Fc[11]CPP** was separated as an orange solid (7 mg, 7 %). $^1$H NMR (600 MHz, Chloroform-d) δ 7.64 – 7.62 (m, 14H), 7.61 (s, 12H), 7.60 (s, 10H), 7.45 (d, J = 8.0 Hz, 4H), 7.39 (d, J = 8.0 Hz, 4H), 4.41 (s, 4H), 4.33 – 4.30 (m, 4H). $^{13}$C NMR (151 MHz, Chloroform-d) δ 139.5, 139.1, 138.9, 138.6, 138.5, 138.3, 127.7, 127.7, 127.6, 127.6, 127.5, 127.4, 127.1, 127.0. HRMS (ESI) m/z calculated for $C_{76}H_{52}Fe$ $[M]^+$ 1020.3413, Found: 1020.3413.

## 7. X-Ray Crystallography

Table S4. Crystallographic Data for **1,3-FcBr** and **main-Fc[11]CPP**

| **Compound** | **1,3-FcBr** | **main-Fc[11]CPP** |
|---|---|---|
| CCDC Deposition number | | 2494120 |
| Empirical formula | $C_{22}H_{16}Br_2Fe$ | $C_{76}H_{52}Fe$ |
| Formula weight | 496.02 | 1021.10 |
| Crystal system | orthorhombic | triclinic |
| Temperature/K | 293(2) | 100.15 |
| Space group | $Pca2_1$ | P-1 |
| α/° | 7.7343(6) | 109.6990(10) |
| β/° | 11.0932(8) | 112.891(2) |
| γ/° | 21.7094(14) | 92.4700(10) |
| a/Å | 90 | 18.3002(3) |
| b/Å | 90 | 19.1527(3) |
| c/Å | 90 | 21.2204(4) |
| Z | 4 | 2 |
| Volume/Å$^3$ | 1862.6(2) | 6319.5(2) |
| $\rho_{calc}$ g/cm$^3$ | 1.769 | 1.207 |
| *F*(000) | 976.0 | 2400.0 |
| μ/mm$^{-1}$ | 5.101 | 2.050 |
| Radiation | Mo Kα (λ = 0.71073) | GaKα (λ = 1.3405) |
| Crystal size/mm$^3$ | 0.05 × 0.03 × 0.02 | 0.05 × 0.05 × 0.04 |
| 2$\Theta$ range for data collection/° | 6.422 to 50.054 | 4.256 to 110.822 |
| Reflections collected | 9495 | 79160 |
| Index ranges | -8 ≤ h ≤ 9, -12 ≤ k ≤ 13, -25 ≤ l ≤ 25 | -22 ≤ h ≤ 22, -21 ≤ k ≤ 23, -25 ≤ l ≤ 25 |
| Independent reflections | 3162 [$R_{int}$ = 0.0282, $R_{sigma}$ = 0.0359] | 23942 [$R_{int}$ = 0.0729, $R_{sigma}$ = 0.0740] |
| Data/restraints/parameters | 3162/1/227 | 23942/36/1505 |
| Goodness-of-fit on $F^2$ | 1.024 | 1.042 |
| Final R indexes [I>=2σ (I)] | *$R_1$ = 0.0294, w$R_2$ = 0.0543* | $R_1$ = 0.0697, w$R_2$ = 0.1834 |
| Final R indexes [all data] | *$R_1$ = 0.0392, w$R_2$ = 0.0565* | $R_1$ = 0.0945, w$R_2$ = 0.1965 |
| Largest diff. peak/hole / e Å$^{-3}$ | 0.31/-0.28 | 0.85/-0.90 |

## 8. UV/vis spectrum of compounds 1,1′-FcCl, 1,3-FcCl, 1,1′-FcBr and 1,3-FcBr

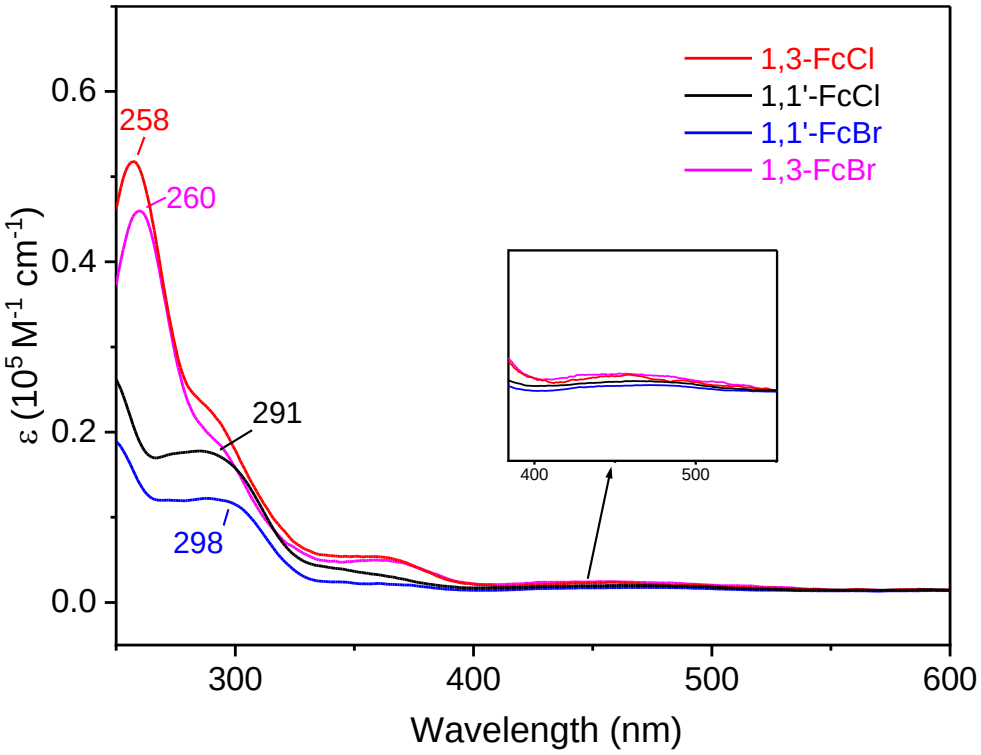


**Figure S2.** UV/vis spectrum of compounds **1,1′-FcCl**, **1,3-FcCl**, **1,1′-FcBr** and **1,3-FcBr**.

## 9. Solvatochromic analysis of main-Fc[11]CPP

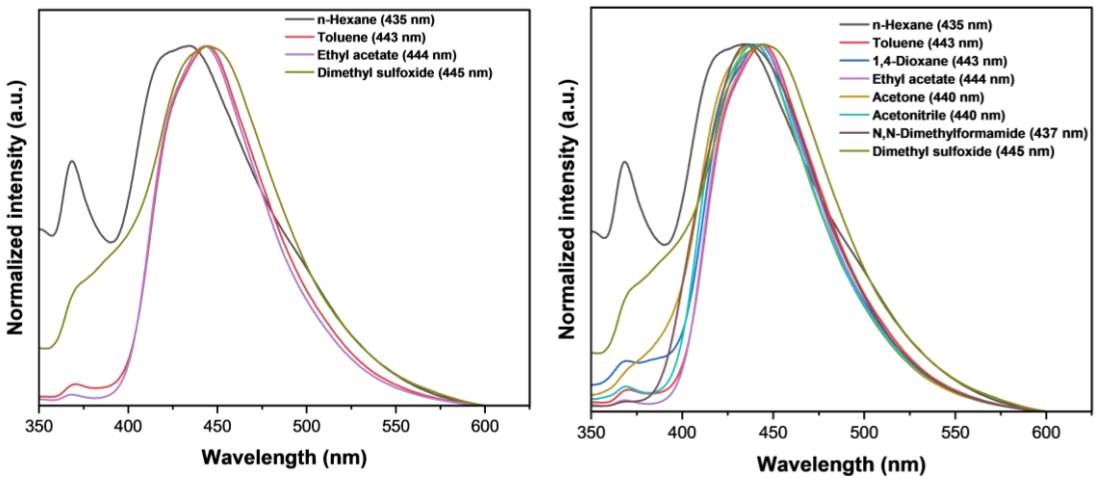


**Figure S3.** A comparative solvatochromic analysis of **main-Fc[11]CPP** in four versus eight solvents of varying polarity.

## 10. The cyclic voltammetry (CV) and differential pulse voltammetry (DPV)

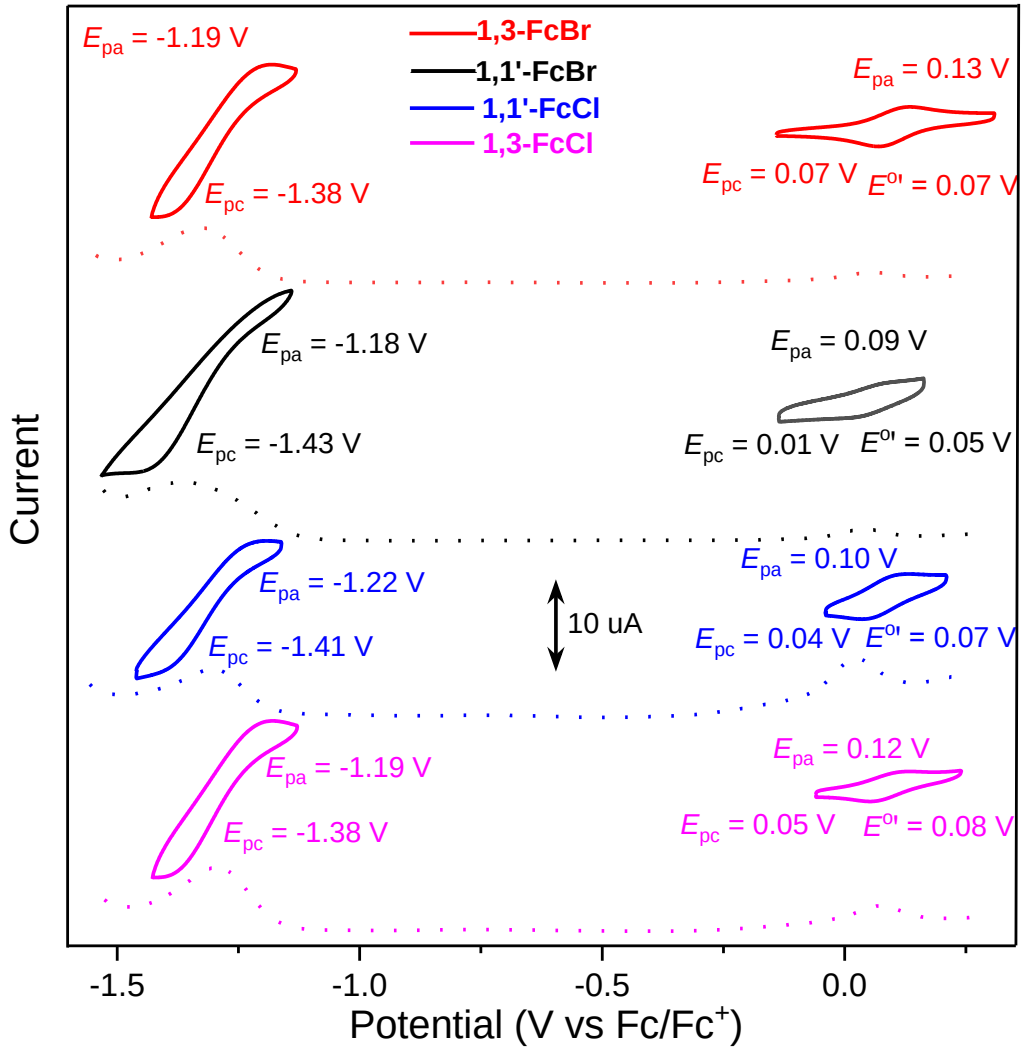


**Figure S4**. The CV (solid line) and DPV (short dashed line) curves of compounds **1,1′-FcCl**, **1,3-FcCl**, **1,1′-FcBr** and **1,3-FcBr** in dichloromethane solution (0.1 M *n*-$Bu_4NPF_6$) at room temperature. $E_{pa}$ and $E_{pc}$ correspond to the anodic peak potential and cathodic peak potential, respectively, $E^{o'} = (E_{pa} + E_{pc})/2$

## 11. DFT Calculation

The frontline molecular orbitals of **1,1′-FcCl**, **1,3-FcCl**, **1,1′-FcBr,** and **1,3-FcBr** were calculated at the B3LYP/def2-TZVP level with the Gaussian 16 program. [13] [12] [13] [13] [12] Spin densities were drawn by combining the Multiwfn 3.8[14] and the VMD programs.[15]

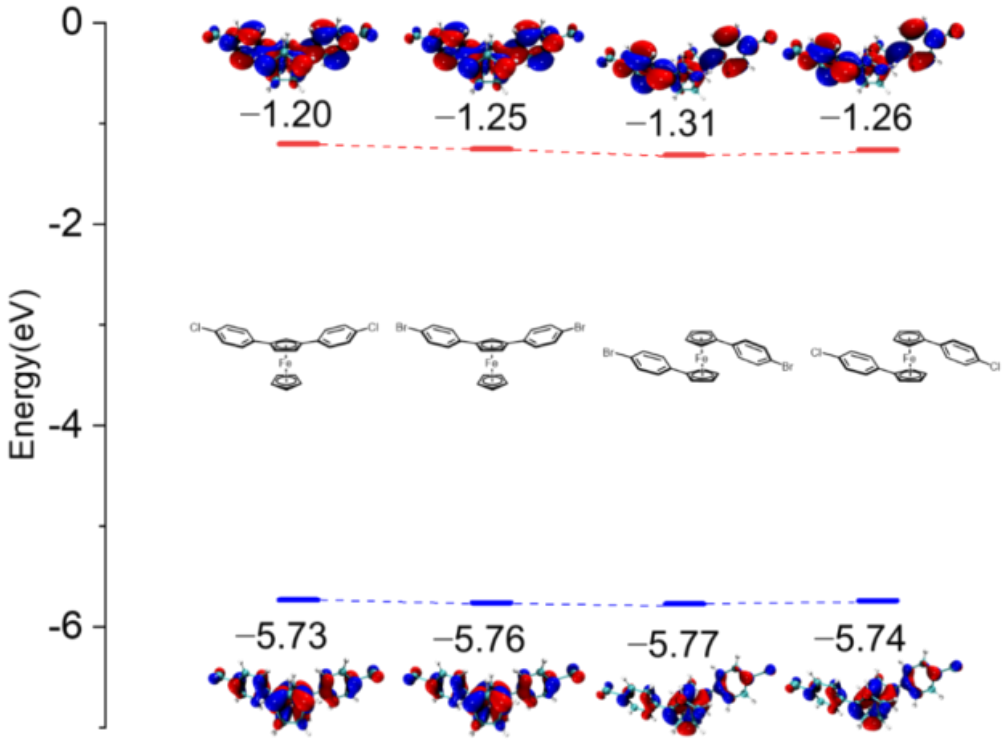


**Figure S5.** Frontline molecular orbitals and energy levels of compounds

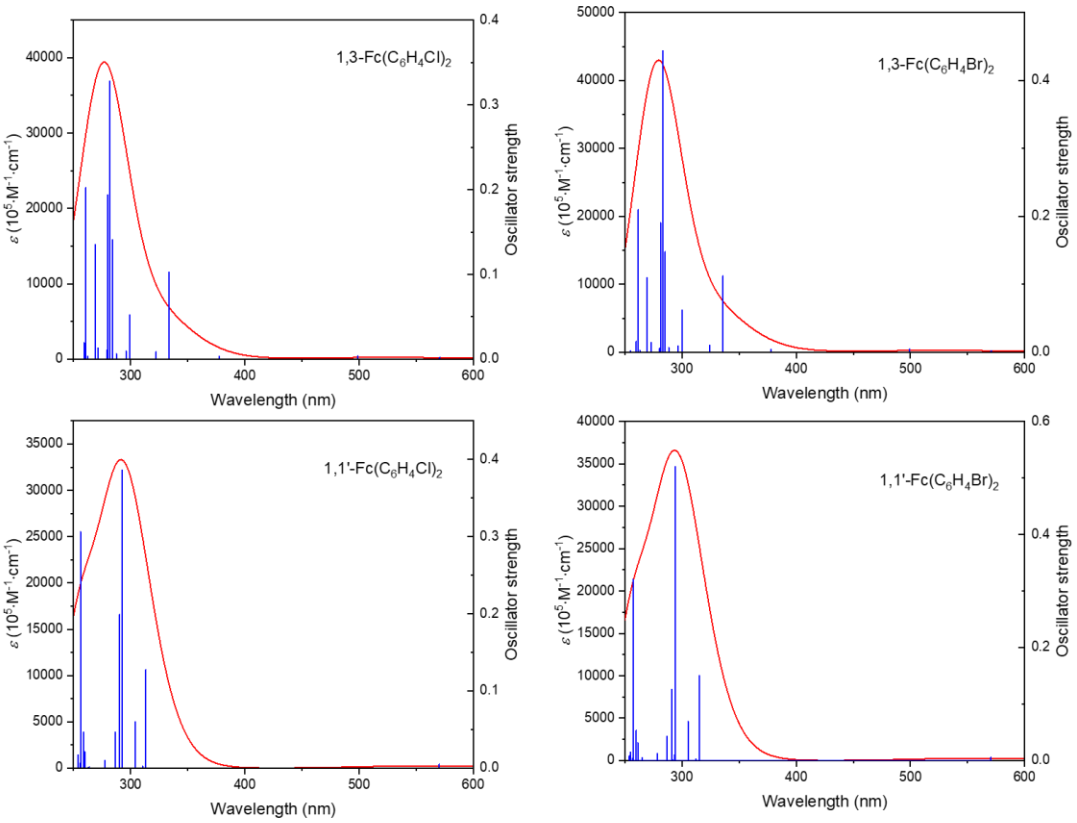


**Figure S6.** The UV visible absorption spectrum (red) and oscillator intensity (blue) of the simulated compound calculated by TD-DFT at the B3LYP/def2-TZVP level.

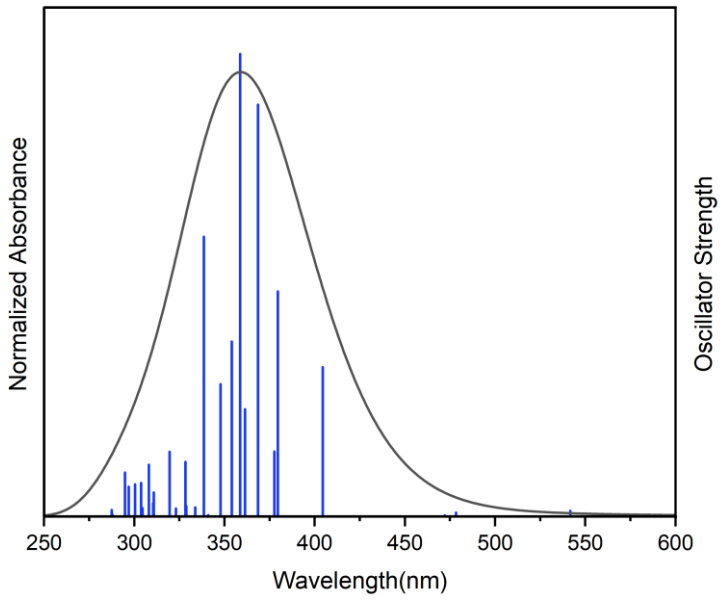


**Figure S7 Main-Fc[11]CPP** calculated TD-DFT absorption spectrum.

Table S5 Electronic transitions of **Main-Fc[11]CPP** calculation via TD-DFT (those with oscillator strengths less than 0.1 are not listed in the table).

| **Excited states** | **Energy (eV)** | **Wavelength [nm]** | **Oscillator strength (f)** | **Contribution** |
|---|---|---|---|---|
| S5 | 3.0663 | 404.34 | 0.3482 | H-1 → L 71.5%, H → L 9.0%, H-2 → L 8.3% |
| S6 | 3.2672 | 379.48 | 0.5246 | H → L 54.7%, H-1 → L 8.2%, H → L+1 6.1% |
| S7 | 3.2829 | 377.67 | 0.1517 | H-2 → L 14.8%, H → L+1 14.4%, H → L 8.4%, H-2 → L+2 5.9% |
| S8 | 3.3641 | 368.55 | 0.9598 | H-1 → L+1 27.8%, H → L 11.8%, H-3 → L 9.3%, H-2 → L+1 6.1% |
| S9 | 3.4313 | 361.33 | 0.2502 | H-2 → L 39.8%, H → L+1 37.0%, H-1 → L 8.1% |
| S10 | 3.4577 | 358.57 | 1.0775 | H-1 → L+1 36.0%, H-2 → L+1 11.4%, H-2 → L 10.4%, H → L 6.5%, H → L+2 5.3% |

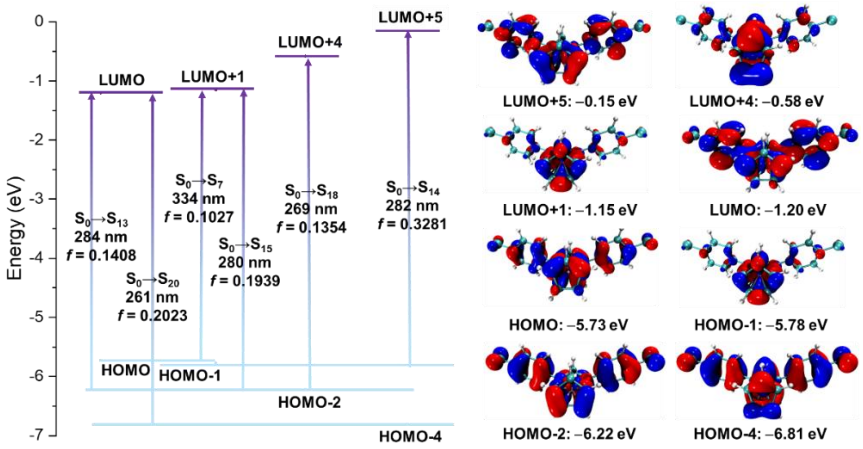


**Figure S8.** Frontier molecular orbitals and main molecular orbital transitions of compound **1,3-FcCl** calculated at the B3LYP/def2-TZVP level of theory.

**Table S6** Electronic transitions of **1,3-FcCl** calculation

| Excited states | Energy (eV) | Wavelength (nm) | Osc. Strength | Description |
|---|---|---|---|---|
| S1 | 2.1732 | 570.51 | 0.0020 | H-1 -> L 42.2%, H -> L+4 28.0%, H-1 -> L+5 19.3% |
| S3 | 2.4847 | 498.99 | 0.0039 | H-3 -> L 27.2%, H -> L+4 25.7%, H-3 -> L+5 15.3%, H-1 -> L 10.9% |
| S5 | 3.2851 | 377.41 | 0.0034 | H-3 -> L 32.3%, H -> L+4 21.9%, H-1 -> L 20.0%, H-3 -> L+5 12.0% |
| S7 | 3.7158 | 333.67 | 0.1027 | H -> L+1 85.6%, H -> L+4 7.8% |
| S8 | 3.8464 | 322.34 | 0.0090 | H-1 -> L+1 77.1%, H-1 -> L+4 8.6% |
| S9 | 4.1442 | 299.18 | 0.0520 | H-1 -> L+2 70.8%, H-1 -> L+5 17.2%, H-1 -> L 7.6% |
| S10 | 4.1901 | 295.90 | 0.0096 | H -> L+2 71.2%, H-2 -> L 20.8% |
| S11 | 4.2637 | 290.79 | 0.0001 | H -> L+3 85.6%, H -> L+4 7.0% |
| S12 | 4.3099 | 287.67 | 0.0062 | H-1 -> L+3 83.8%, H-1 -> L+4 7.1% |
| S13 | 4.3639 | 284.11 | 0.1408 | H-2 -> L 58.8%, H -> L+2 13.7%, H -> L 9.2% |
| S14 | 4.3982 | 281.90 | 0.3281 | H-1 -> L+5 32.7%, H-2 -> L+1 26.7%, H-1 -> L+2 19.2%, H-1 -> L 10.3% |
| S15 | 4.4273 | 280.04 | 0.1939 | H-2 -> L+1 49.5%, H-1 -> L+5 18.1%, H-2 -> L+4 8.8%, H-1 -> L+2 7.3%, H-1 -> L 5.8% |
| S16 | 4.4388 | 279.32 | 0.0106 | H -> L+5 66.3%, H -> L 19.9% |
| S17 | 4.5671 | 271.47 | 0.0132 | H-3 -> L+1 81.4%, H-3 -> L+4 5.2% |
| S18 | 4.6037 | 269.31 | 0.1354 | H-2 -> L+4 51.0%, H-2 -> L+3 23.1%, H-2 -> L+1 15.3% |
| S19 | 4.7242 | 262.44 | 0.0033 | H-2 -> L+2 84.5% |
| S20 | 4.7559 | 260.70 | 0.2023 | H-4 -> L 71.4%, H-3 -> L 8.7%, H-5 -> L 7.6% |

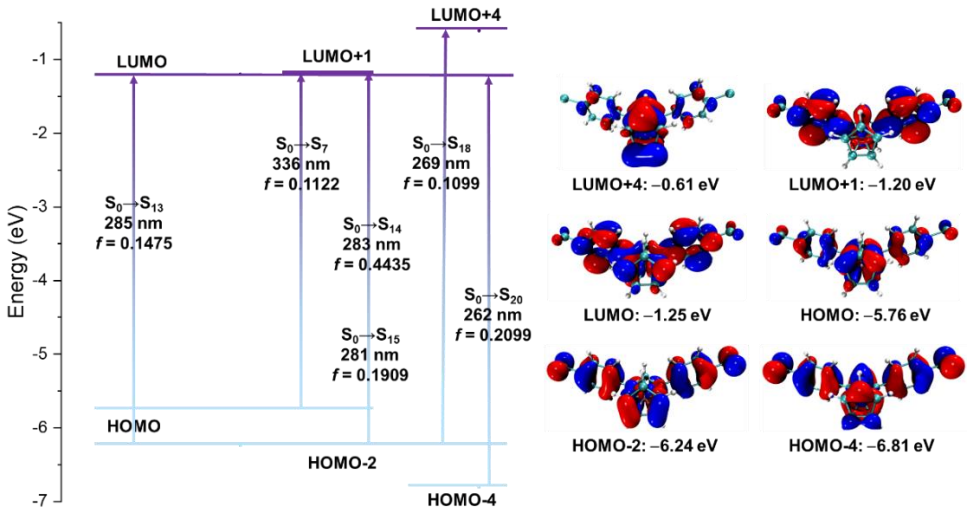


**Figure S9.** Frontier molecular orbitals and main molecular orbital transitions of compound **1,3-FcBr** calculated at the B3LYP/def2-TZVP level of theory

**Table S7** Electronic transitions of **1,3-FcBr** calculation

| Excited states | Energy (eV) | Wavelength (nm) | Osc. Strength | Description |
|---|---|---|---|---|
| S1 | 2.1720 | 570.83 | 0.0022 | H-1 -> L 41.9%, H -> L+4 27.6%, H-1 -> L+7 18.7% |
| S7 | 3.6924 | 335.78 | 0.1122 | H -> L+1 85.8%, H -> L+4 7.7% |
| S8 | 3.8254 | 324.11 | 0.0098 | H-1 -> L+1 77.5%, H-1 -> L+4 8.6% |
| S9 | 4.1313 | 300.11 | 0.0616 | H-1 -> L+2 68.8%, H-1 -> L+7 16.9%, H-1 -> L 8.5% |
| S10 | 4.1835 | 296.36 | 0.0089 | H -> L+2 71.5%, H-2 -> L 20.3% |
| S11 | 4.2557 | 291.34 | 0.0000 | H -> L+3 85.5%, H -> L+4 6.4% |
| S12 | 4.3006 | 288.30 | 0.0068 | H-1 -> L+3 83.8%, H-1 -> L+4 6.6% |
| S13 | 4.3500 | 285.02 | 0.1475 | H-2 -> L 58.1%, H -> L+2 12.0%, H -> L 11.0% |
| S14 | 4.3790 | 283.13 | 0.4435 | H-2 -> L+1 36.0%, H-1 -> L+7 23.7%, H-1 -> L+2 18.0%, H-1 -> L 8.3%, H -> L+3 5.6% |
| S15 | 4.4125 | 280.98 | 0.1909 | H-2 -> L+1 45.5%, H-1 -> L+7 21.1%, H-1 -> L+2 10.4%, H-1 -> L 7.3% |
| S16 | 4.4220 | 280.38 | 0.0064 | H -> L+7 59.3%, H -> L 18.5%, H -> L+2 5.9%, H -> L+5 5.8% |
| S17 | 4.5432 | 272.90 | 0.0137 | H-3 -> L+1 80.8%, H-4 -> L+1 5.1% |
| S18 | 4.6023 | 269.40 | 0.1099 | H-2 -> L+4 54.1%, H-2 -> L+3 24.1%, H-2 -> L+1 10.2%, H -> L+4 5.4% |
| S19 | 4.7145 | 262.98 | 0.0024 | H-2 -> L+2 83.9% |
| S20 | 4.7395 | 261.60 | 0.2099 | H-4 -> L 68.2%, H-3 -> L 10.1%, H-5 -> L 9.6% |

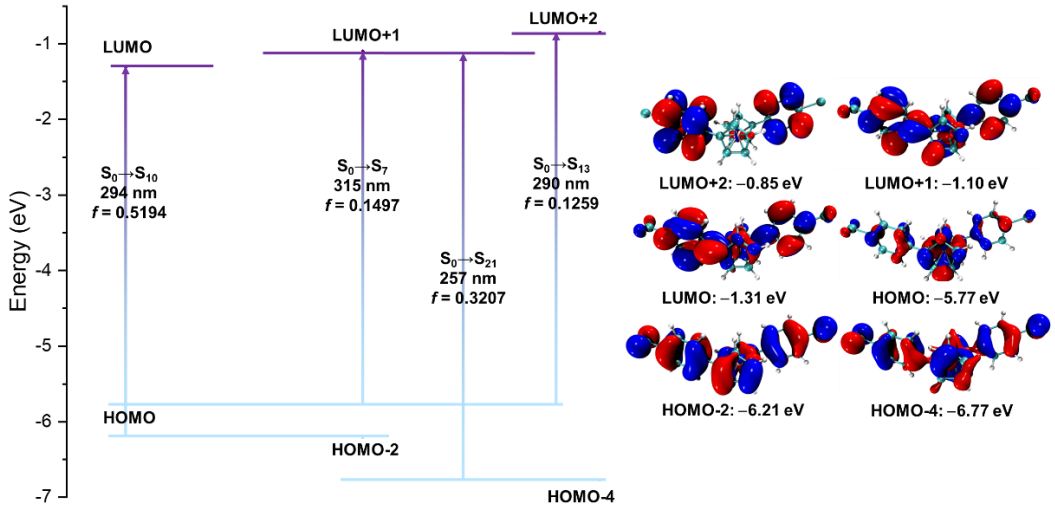


**Figure S10.** Frontier molecular orbitals and main molecular orbital transitions of compound **1,1'-FcBr** calculated at the B3LYP/def2-TZVP level of theory

**Table S8** Electronic transitions of **1,1'-FcBr** calculation

| Excited states | Energy (eV) | Wavelength (nm) | Osc. Strength | Description |
|---|---|---|---|---|
| S2 | 2.1736 | 570.41 | 0.0061 | H-1 -> L 34.8%, H -> L+4 26.6%, H-1 -> L+7 16.6%, H -> L+1 9.7%, H-1 -> L+5 6.5% |
| S7 | 3.9358 | 315.02 | 0.1497 | H -> L+1 63.1%, H -> L+4 27.4% |
| S8 | 3.9732 | 312.05 | 0.0039 | H-1 -> L+1 50.7%, H-1 -> L+4 15.9%, H -> L 9.5%, H -> L+7 9.3% |
| S9 | 4.0631 | 305.15 | 0.0691 | H-1 -> L+7 36.0%, H-1 -> L 24.8%, H-1 -> L+2 16.7%, H-1 -> L+5 14.7% |
| S10 | 4.2175 | 293.98 | 0.5194 | H-2 -> L 81.3%, H -> L+3 9.3% |
| S11 | 4.2265 | 293.35 | 0.0096 | H -> L+2 62.5%, H-1 -> L+3 13.2%, H-1 -> L+1 6.5% |
| S12 | 4.2561 | 291.31 | 0.0020 | H -> L+7 29.1%, H -> L+2 23.7%, H -> L 18.7%, H -> L+5 12.9%, H-1 -> L+1 5.1% |
| S13 | 4.2613 | 290.95 | 0.1259 | H -> L+3 67.2%, H-1 -> L+2 12.7%, H-2 -> L 11.6% |
| S14 | 4.3216 | 286.89 | 0.0428 | H-1 -> L+2 67.0%, H -> L+3 15.4%, H-1 -> L+7 7.9% |
| S15 | 4.3363 | 285.92 | 0.0000 | H-1 -> L+3 78.8%, H-1 -> L+4 7.7% |
| S16 | 4.4593 | 278.04 | 0.0126 | H-2 -> L+1 72.6%, H-2 -> L+4 15.0% |
| S21 | 4.8259 | 256.91 | 0.3204 | H-4 -> L+1 45.7%, H-4 -> L+4 13.9%, H-3 -> L+1 11.2%, H-2 -> L+2 6.6%, H-3 -> L+4 5.8% |

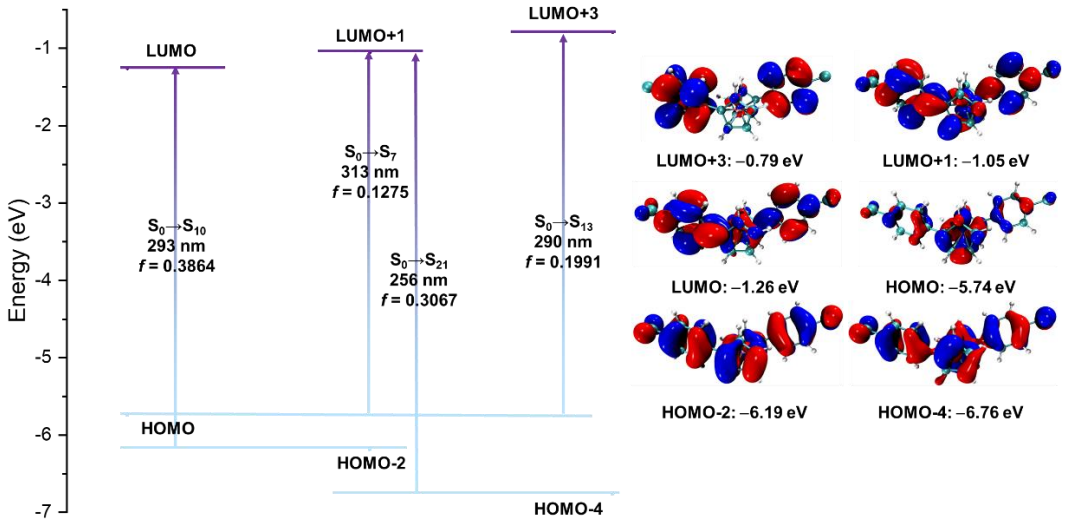


**Figure S11.** Frontier molecular orbitals and main molecular orbital transitions of compound **1,1'-FcCl** calculated at the B3LYP/def2-TZVP level of theory

**Table S9** Electronic transitions of **1,1'-FcCl** calculation

| Excited states | Energy (eV) | Wavelength (nm) | Osc. Strength | Description |
|---|---|---|---|---|
| S2 | 2.1750 | 570.04 | 0.0055 | H-1 -> L 34.8%, H -> L+4 27.1%, H-1 -> L+5 22.7%, H -> L+1 10.3% |
| S7 | 3.9582 | 313.23 | 0.1275 | H -> L+1 61.9%, H -> L+4 29.0% |
| S10 | 4.2356 | 292.72 | 0.3864 | H-2 -> L 69.5%, H -> L+3 19.1% |
| S11 | 4.2362 | 292.68 | 0.0085 | H -> L+2 73.5%, H-1 -> L+3 11.0% |
| S12 | 4.2714 | 290.27 | 0.0028 | H -> L+5 45.9%, H -> L 20.3%, H -> L+2 12.4%, H-1 -> L+1 6.6%, H-1 -> L+3 5.6% |
| S13 | 4.2720 | 290.23 | 0.1991 | H -> L+3 57.7%, H-2 -> L 23.0%, H-1 -> L+2 11.2% |
| S14 | 4.3295 | 286.37 | 0.0468 | H-1 -> L+2 65.7%, H -> L+3 15.3%, H-1 -> L+5 12.0% |
| S16 | 4.4678 | 277.51 | 0.0096 | H-2 -> L+1 70.9%, H-2 -> L+4 16.9% |
| S17 | 4.6974 | 263.94 | 0.0016 | H-4 -> L 48.8%, H-2 -> L+3 18.4%, H-3 -> L 7.9%, H-5 -> L 6.0% |
| S18 | 4.7207 | 262.64 | 0.0005 | H-2 -> L+2 72.7%, H-4 -> L+1 6.2%, H-6 -> L 5.5% |
| S19 | 4.7709 | 259.88 | 0.0212 | H-3 -> L+1 56.6%, H-3 -> L+4 22.0%, H-4 -> L+1 9.1% |
| S20 | 4.7915 | 258.76 | 0.0466 | H-2 -> L+3 51.9%, H-4 -> L 13.0%, H-7 -> L 6.2%, H-3 -> L 5.1% |
| S21 | 4.8403 | 256.15 | 0.3067 | H-4 -> L+1 44.5%, H-4 -> L+4 16.9%, H-3 -> L+1 11.9%, H-2 -> L+2 6.2% |

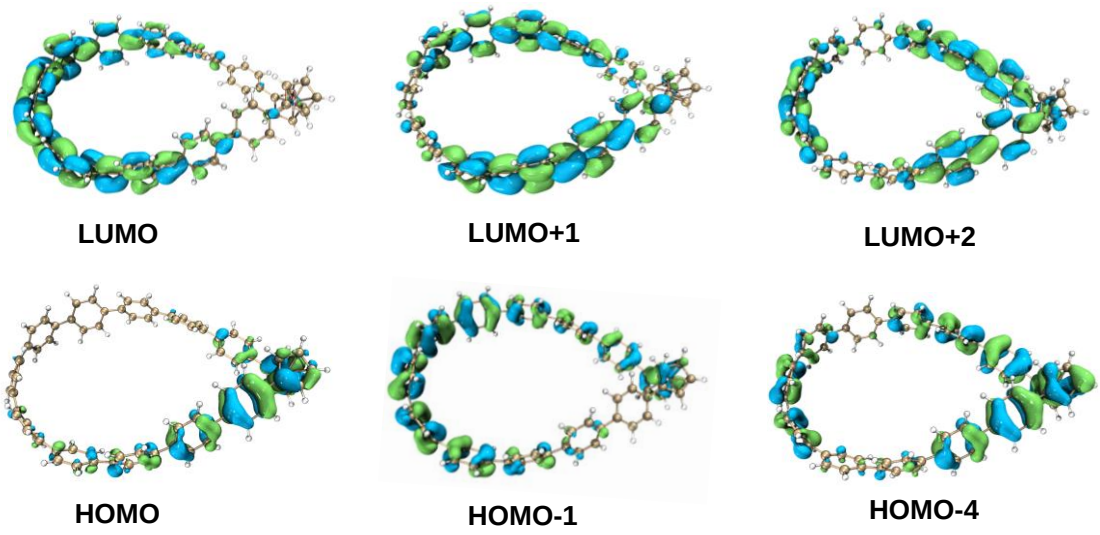


**Figure S12** Frontier molecular orbitals of **main-Fc[11]CPP** calculated at the B3LYP/6-31G(d)/SDD level of theory.

## 12. Cartesian coordinates of optimized structures

**main-Fc[11]CPP** (B3LYP/6-31G(d)/SDD)

| | | | | | | | |
|---|---|---|---|---|---|---|---|
| C | -7.6207 | -0.9676 | 2.6816 | C | 3.3565 | -5.2905 | -4.4982 |
| C | -8.5407 | -0.1297 | 3.8388 | C | 4.6693 | -5.1745 | -4.2356 |
| C | -7.7677 | 1.3449 | 4.1752 | C | 5.2223 | -5.5702 | -3.0709 |
| C | -6.3362 | 1.2493 | 3.2724 | C | 4.3792 | -6.2968 | -2.3083 |
| C | -6.2834 | -0.0473 | 2.1846 | C | 3.0672 | -6.4241 | -2.5774 |
| C | -8.5422 | 2.8384 | 1.9871 | C | 6.4463 | -5.1445 | -2.6522 |
| C | -9.8268 | 1.7569 | 2.2855 | C | 6.9186 | -5.3628 | -1.4077 |
| C | -9.6746 | 0.3646 | 1.3068 | C | 7.9248 | -4.6482 | -0.8731 |
| C | -8.3731 | 0.7437 | 0.2868 | C | 8.5502 | -3.6533 | -1.5355 |
| C | -7.5951 | 2.1825 | 0.7457 | C | 8.2492 | -3.6243 | -2.8499 |
| C | -5.3901 | 2.3737 | 3.1604 | C | 7.2415 | -4.3366 | -3.3829 |
| C | -5.2075 | 3.2069 | 4.1976 | Fe | -8.0118 | 0.9364 | 2.2403 |
| C | -4.2203 | 4.1198 | 4.2015 | H | -8.0851 | -1.7029 | 2.0431 |
| C | -3.3608 | 4.2694 | 3.1712 | H | -9.6106 | -0.2777 | 3.9422 |
| C | -3.606 | 3.4717 | 2.1093 | H | -8.2736 | 2.2475 | 4.4938 |
| C | -4.5557 | 2.524 | 2.121 | H | -5.8461 | -0.041 | 1.197 |
| C | -2.2375 | 5.0328 | 3.2146 | H | -8.1193 | 3.507 | 2.7295 |
| C | -1.6686 | 5.4293 | 4.3711 | H | -10.3125 | 1.7272 | 3.2561 |
| C | -0.4182 | 5.9237 | 4.4254 | H | -9.9991 | -0.6288 | 1.5907 |
| C | 0.3486 | 6.1154 | 3.3324 | H | -6.5396 | 2.3721 | 0.64 |
| C | -0.3041 | 5.9067 | 2.1706 | H | -5.83 | 3.0934 | 5.1012 |
| C | -1.5328 | 5.3684 | 2.1165 | H | -4.1256 | 4.713 | 5.1248 |
| C | 1.6871 | 6.3545 | 3.3625 | H | -2.9464 | 3.4328 | 1.2282 |
| C | 2.4371 | 6.1554 | 4.4656 | H | -4.5789 | 1.8203 | 1.2742 |
| C | 3.7781 | 6.0562 | 4.4195 | H | -2.1363 | 5.2275 | 5.348 |
| C | 4.4885 | 6.1794 | 3.2793 | H | -0.0262 | 6.094 | 5.4407 |
| C | 3.7514 | 6.6102 | 2.2349 | H | 0.1736 | 6.0251 | 1.186 |

| | | | | | | | |
|---|---|---|---|---|---|---|---|
| C | 2.4103 | 6.6784 | 2.2724 | H | -1.9097 | 5.1625 | 1.1015 |
| C | 5.7764 | 5.7646 | 3.1316 | H | 1.9907 | 5.8995 | 5.4393 |
| C | 6.4159 | 5.0256 | 4.0613 | H | 4.2492 | 5.7562 | 5.3684 |
| C | 7.5127 | 4.2991 | 3.7807 | H | 4.1762 | 6.7886 | 1.2357 |
| C | 8.0751 | 4.2612 | 2.5551 | H | 1.9353 | 6.9338 | 1.3122 |
| C | 7.5886 | 5.2012 | 1.7189 | H | 5.9898 | 4.8341 | 5.0581 |
| C | 6.4826 | 5.9137 | 1.993 | H | 7.8339 | 3.6309 | 4.5943 |
| C | 8.9172 | 3.2754 | 2.1389 | H | 7.9637 | 5.34 | 0.6939 |
| C | 9.4157 | 3.2023 | 0.888 | H | 6.1301 | 6.5438 | 1.1619 |
| C | 9.8956 | 2.0633 | 0.3595 | H | 9.3319 | 4.0321 | 0.1699 |
| C | 9.9095 | 0.8962 | 1.0355 | H | 10.1222 | 2.1312 | -0.7151 |
| C | 9.6695 | 1.0454 | 2.3544 | H | 9.6977 | 0.1995 | 3.058 |
| C | 9.1974 | 2.1873 | 2.8853 | H | 8.9019 | 2.102 | 3.942 |
| C | 9.9813 | -0.3154 | 0.4179 | H | 10.3125 | 0.3837 | -1.589 |
| C | 10.0873 | -0.4595 | -0.9188 | H | 9.7455 | -1.5033 | -2.6546 |
| C | 9.7482 | -1.5926 | -1.5579 | H | 9.149 | -3.441 | 1.0912 |
| C | 9.2715 | -2.6786 | -0.9155 | H | 9.715 | -1.552 | 2.1581 |
| C | 9.4351 | -2.6156 | 0.4219 | H | -6.4956 | 1.3128 | -1.4519 |
| C | 9.777 | -1.4832 | 1.0615 | H | -5.0949 | -0.0779 | -2.6399 |
| C | -7.6026 | -0.235 | -0.5147 | H | -7.1686 | -3.4616 | -1.0709 |
| C | -6.6645 | 0.2272 | -1.3567 | H | -8.6112 | -2.0075 | 0.0679 |
| C | -5.8731 | -0.5964 | -2.0594 | H | -4.2374 | -1.3325 | -3.9349 |
| C | -5.9416 | -1.9402 | -1.9502 | H | -2.4477 | -2.5195 | -4.6003 |
| C | -6.9633 | -2.3855 | -1.1875 | H | -3.5727 | -5.6905 | -1.9912 |
| C | -7.7915 | -1.5638 | -0.5175 | H | -5.3881 | -4.482 | -1.3202 |
| C | -4.9974 | -2.7425 | -2.5089 | H | -0.9992 | -3.6665 | -5.2994 |
| C | -4.143 | -2.3232 | -3.4627 | H | 1.1438 | -4.3163 | -5.4122 |
| C | -3.0891 | -3.0448 | -3.8764 | H | 0.5255 | -6.9329 | -2.1103 |
| C | -2.7646 | -4.2413 | -3.3454 | H | -1.6351 | -6.2686 | -1.9957 |

| | | | | | | | |
|---|---|---|---|---|---|---|---|
| C | -3.688 | -4.7108 | -2.481 | H | 3.0414 | -4.8173 | -5.4407 |
| C | -4.7683 | -4.0059 | -2.0968 | H | 5.2265 | -4.6074 | -4.9962 |
| C | -1.5636 | -4.8323 | -3.5883 | H | 4.6863 | -6.7307 | -1.3446 |
| C | -0.7141 | -4.4222 | -4.5511 | H | 2.4907 | -6.9338 | -1.7902 |
| C | 0.5644 | -4.827 | -4.6285 | H | 6.4145 | -6.0326 | -0.6947 |
| C | 1.1258 | -5.6634 | -3.7317 | H | 8.0935 | -4.8419 | 0.197 |
| C | 0.2298 | -6.2023 | -2.879 | H | 8.7101 | -2.9096 | -3.5481 |
| C | -1.0581 | -5.8172 | -2.8179 | H | 7.0353 | -4.1008 | -4.4378 |
| C | 2.4738 | -5.8245 | -3.6299 | | | | |

## 13. NMR Spectrum

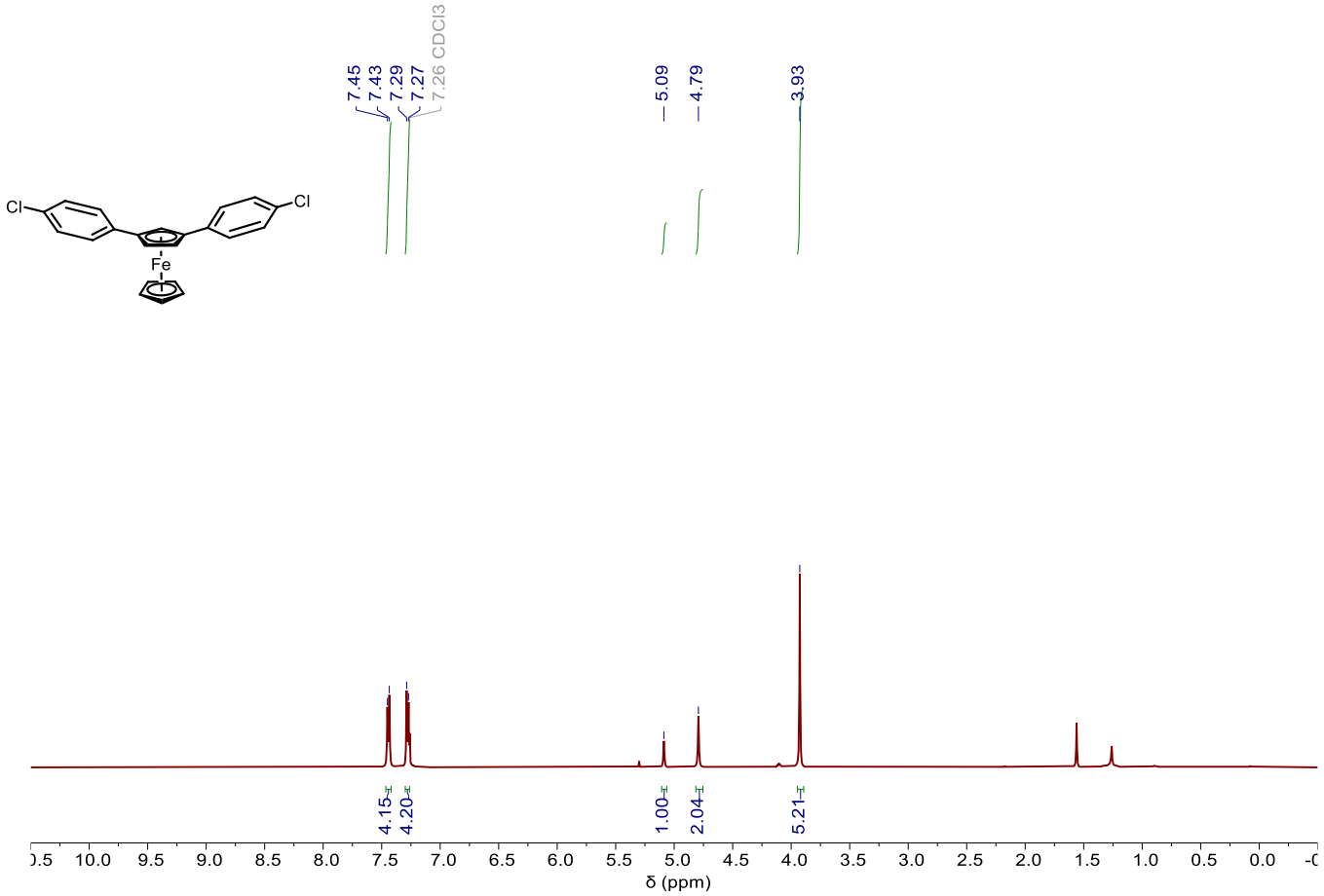


**Figure S13.** $^{1}$H NMR spectrum of **1,3-FcCl** ($CDCl_3$, 600 MHz)

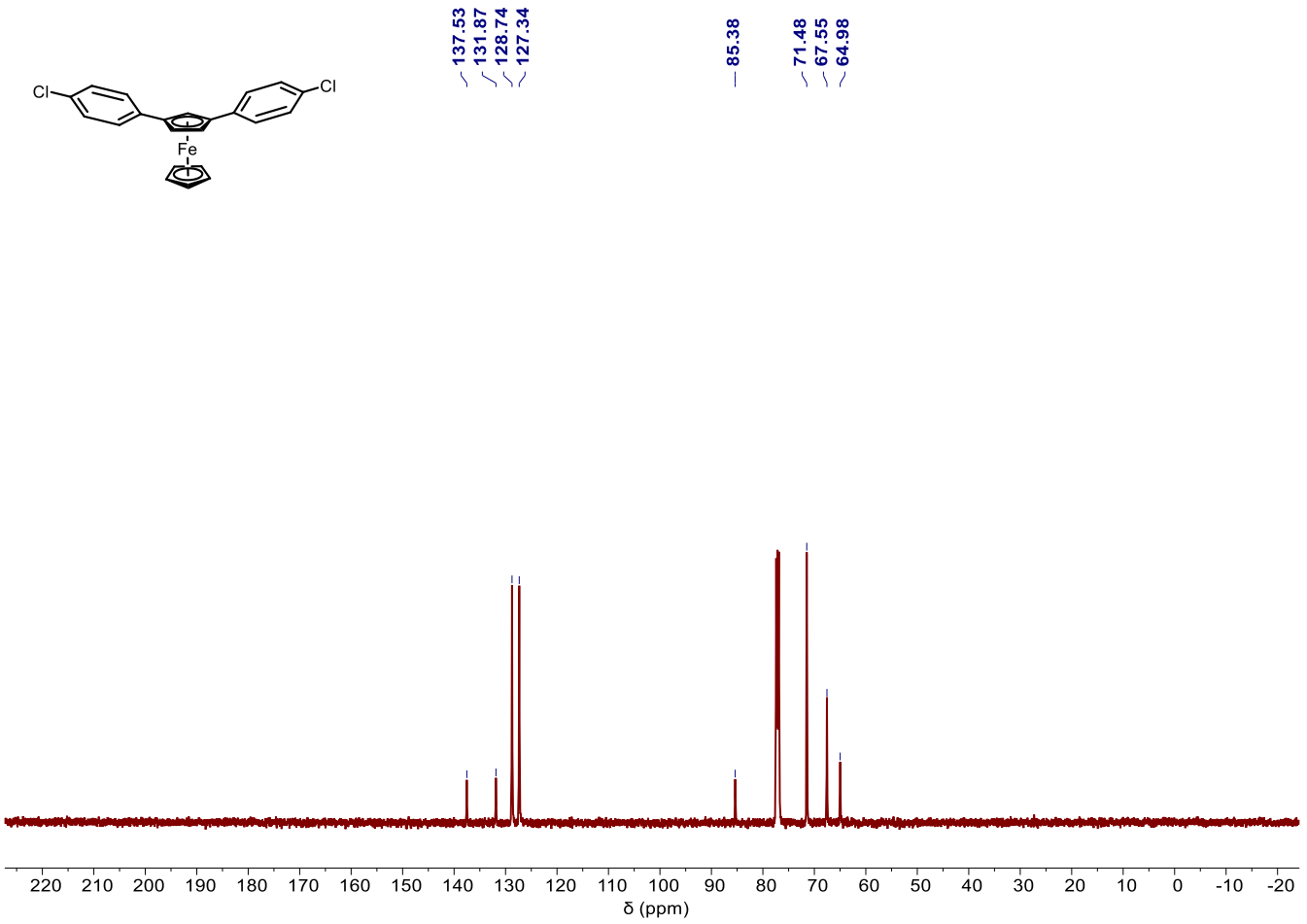


**Figure S14.** $^{13}C$ NMR spectrum of **1,3-FcCl** ($CDCl_3$, 151 MHz)

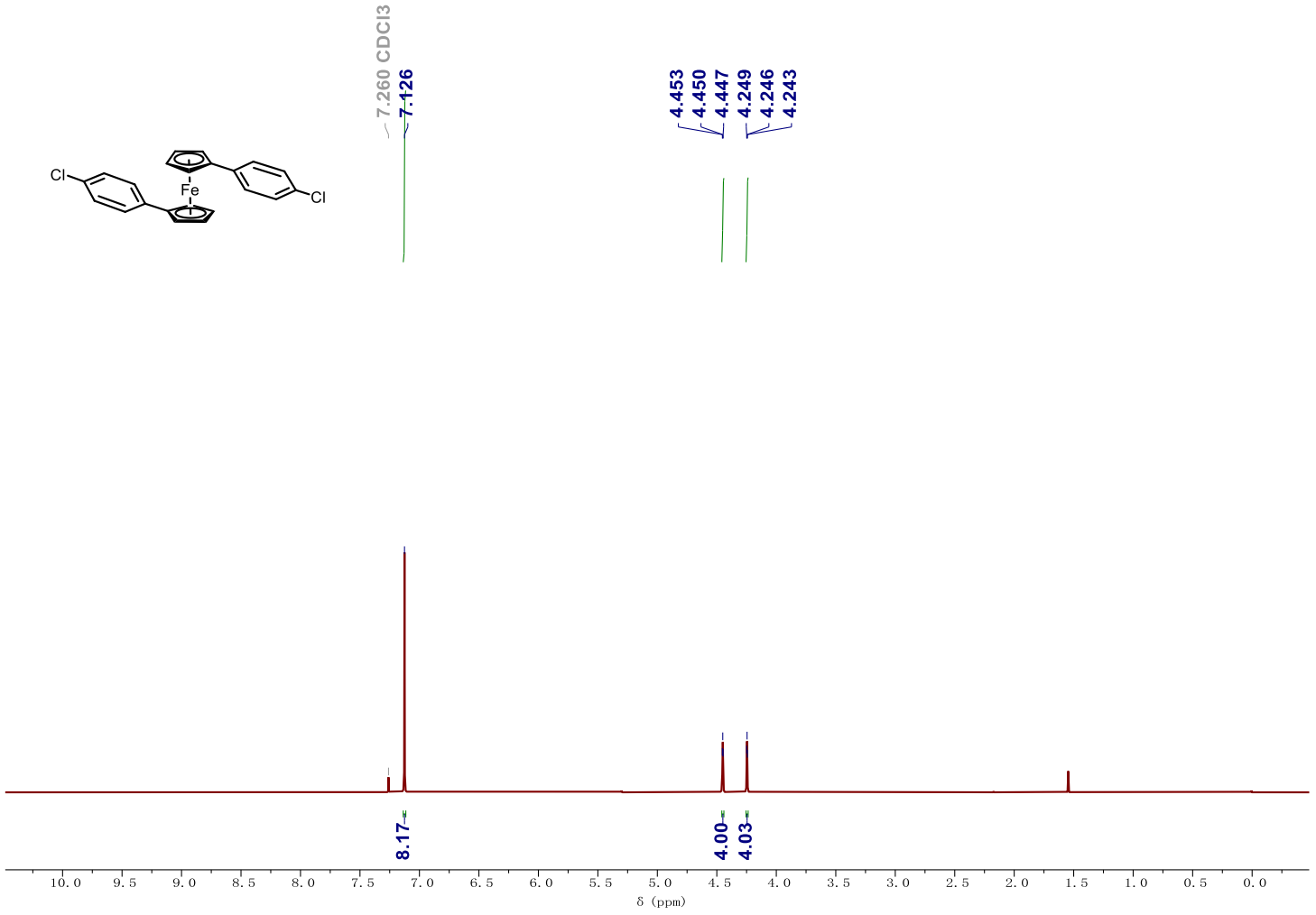


**Figure S15.** $^{1}$H NMR spectrum of **1,1'-FcCl** ($CDCl_3$, 600 MHz)

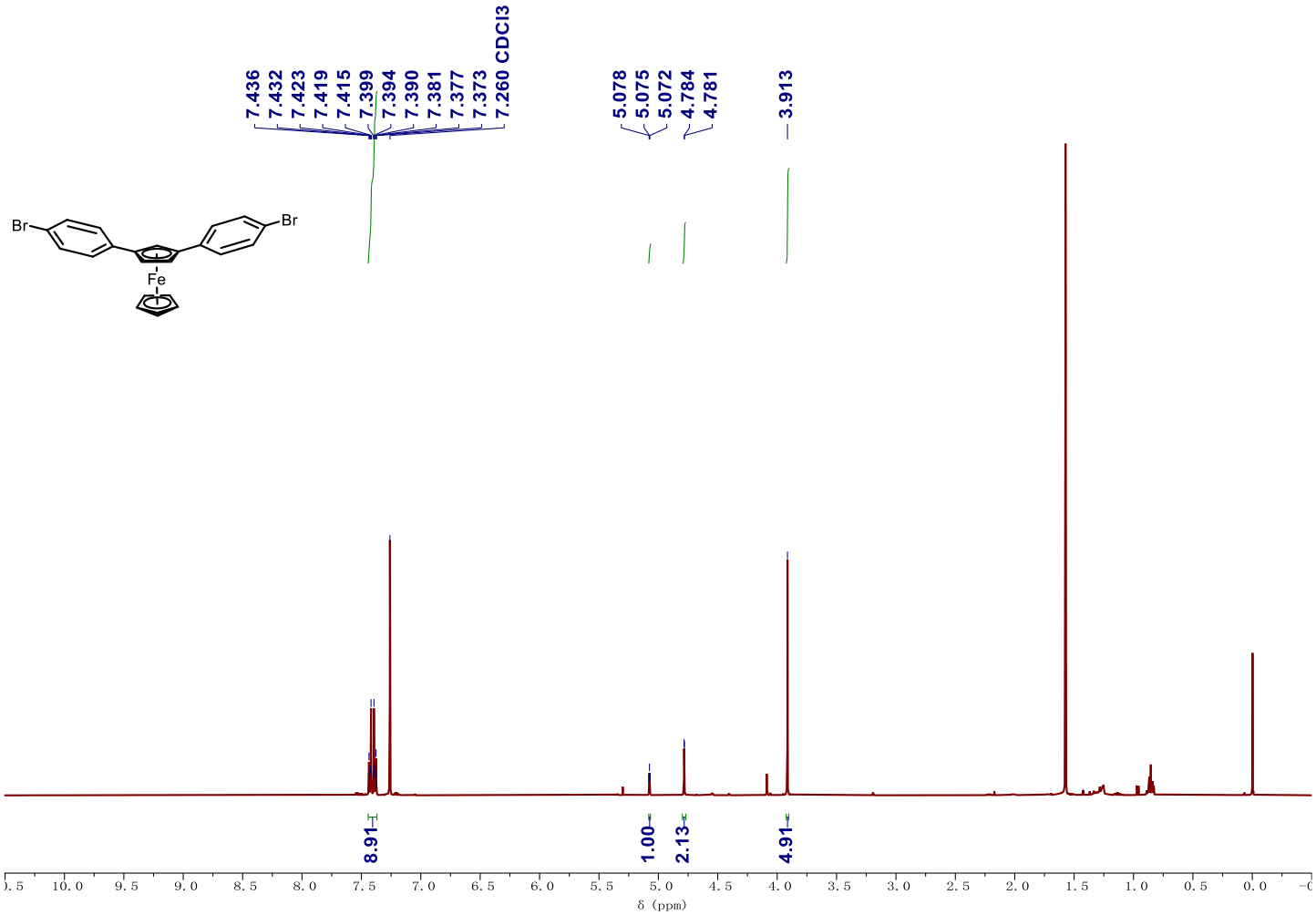


**Figure S16.** $^{1}$H NMR spectrum of **1,3-FcBr** ($CDCl_3$, 600 MHz)

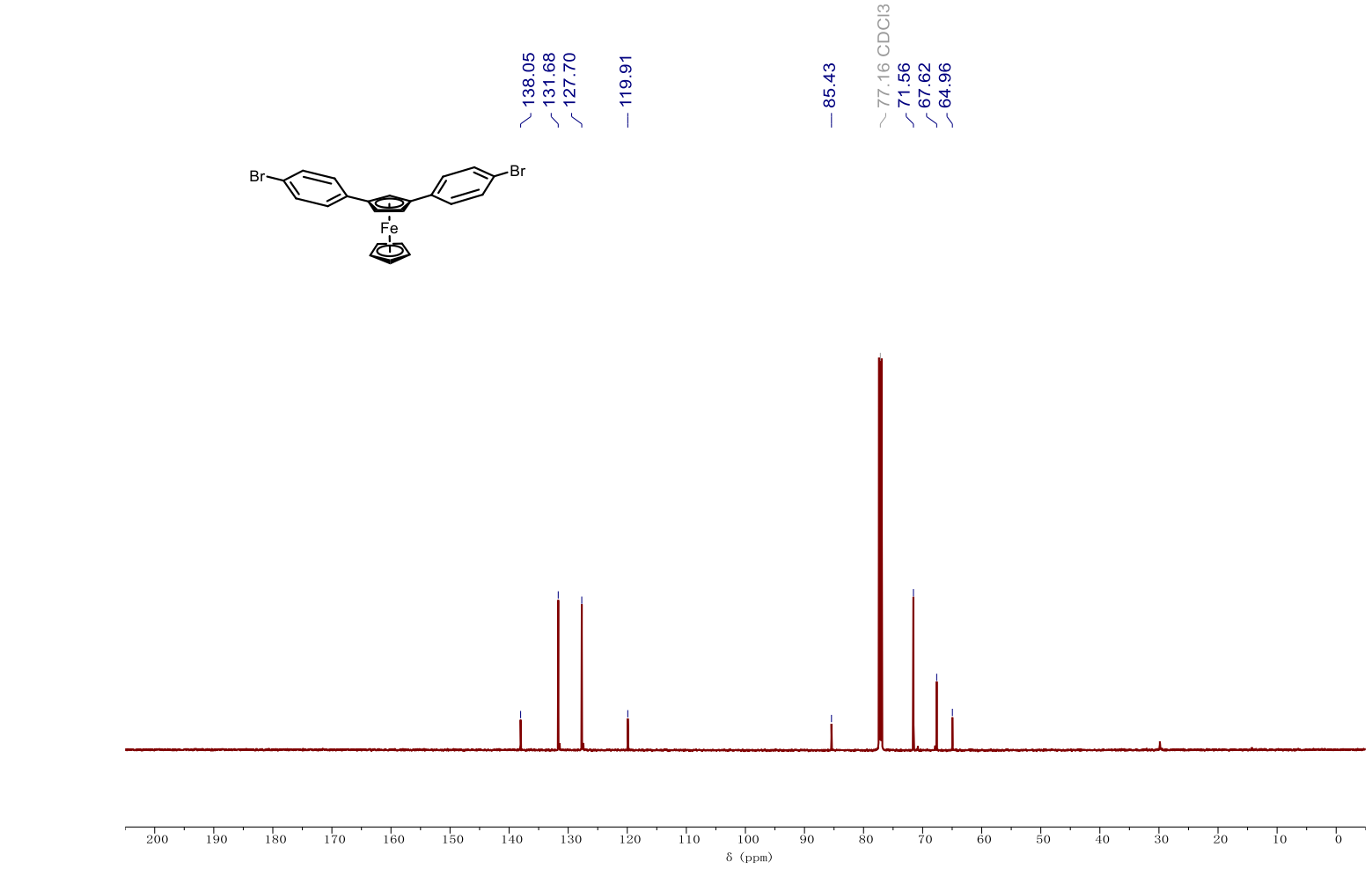


**Figure S17.** $^{13}C$ NMR spectrum of **1,3-FcBr** ($CDCl_3$, 151 MHz)

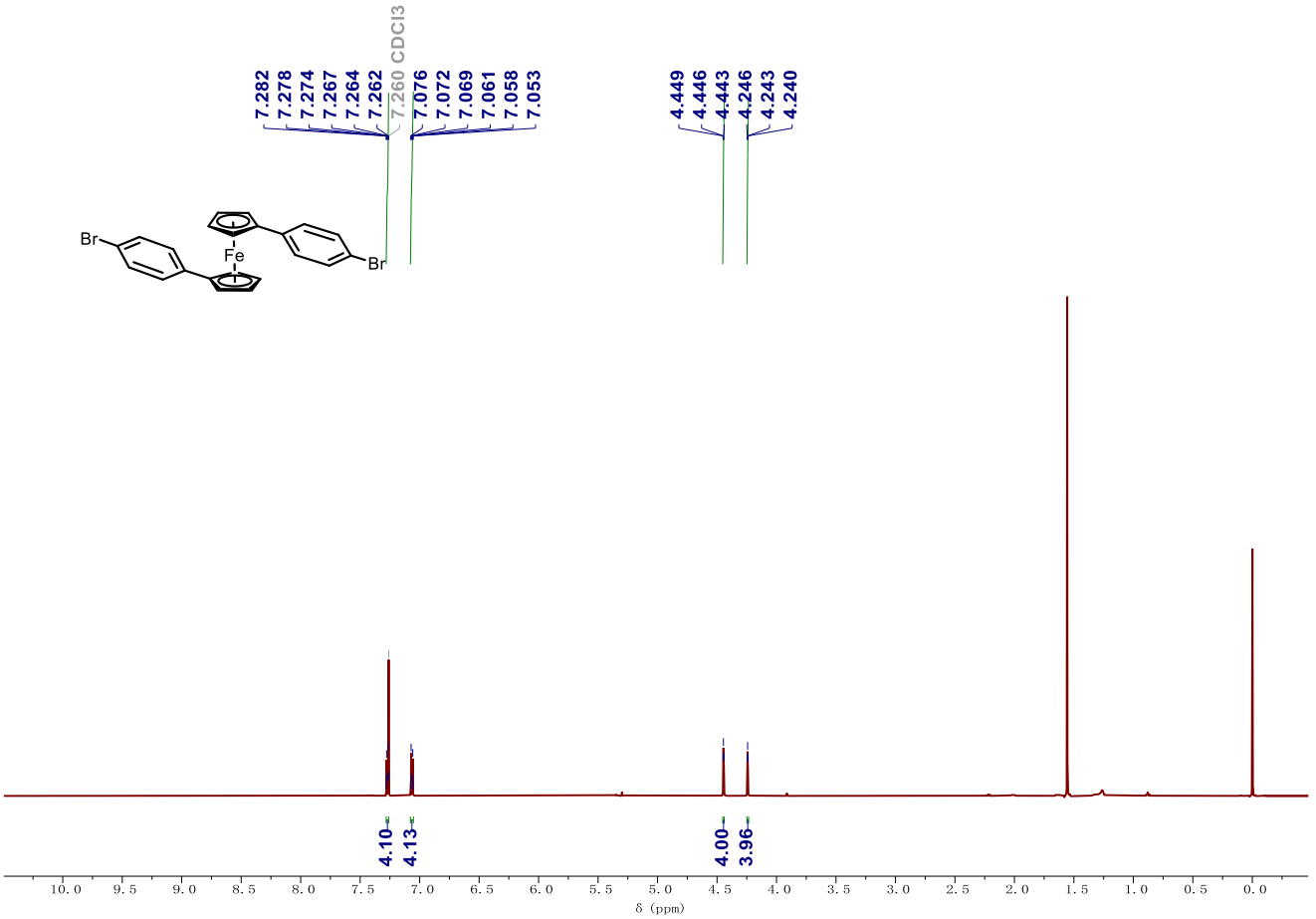


**Figure S18.** $^{1}$H NMR spectrum of **1,1'-FcBr** ($CDCl_3$, 600 MHz)

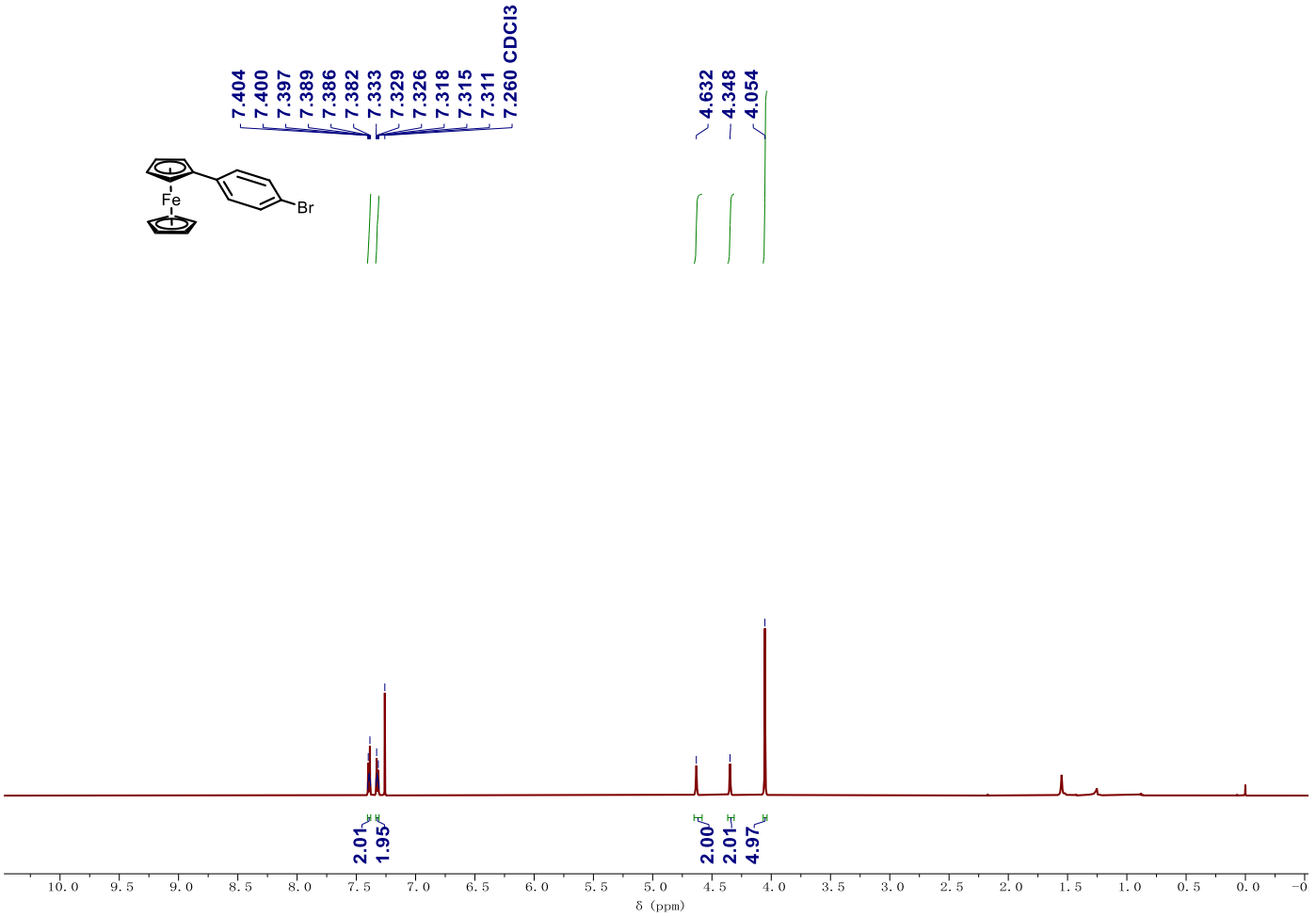


**Figure S19.** $^{1}$H NMR spectrum of **1-FcBr** ($CDCl_3$, 600 MHz)

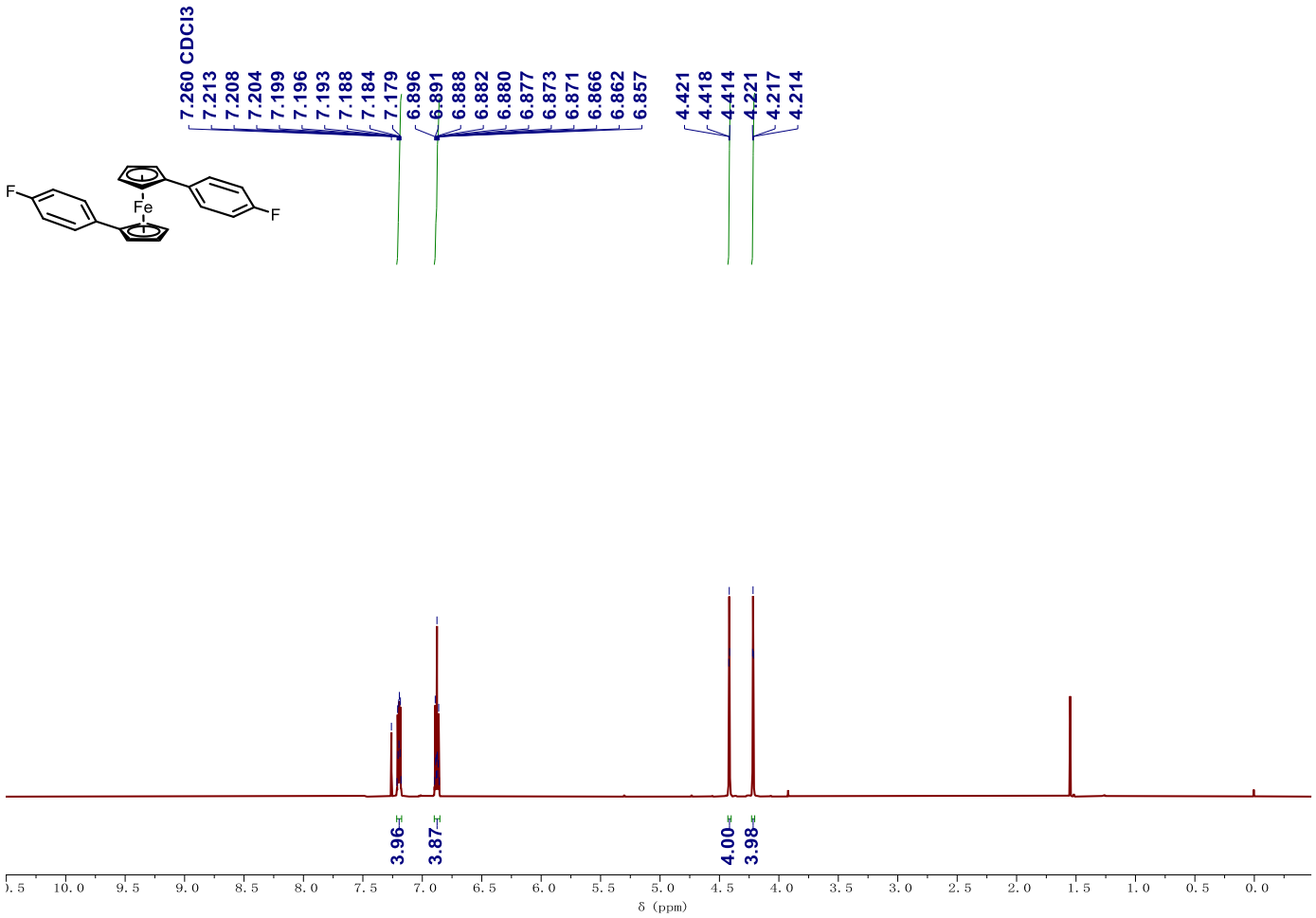


**Figure S20.** $^{1}$H NMR spectrum of **1,1'-FcF** ($CDCl_3$, 600 MHz)

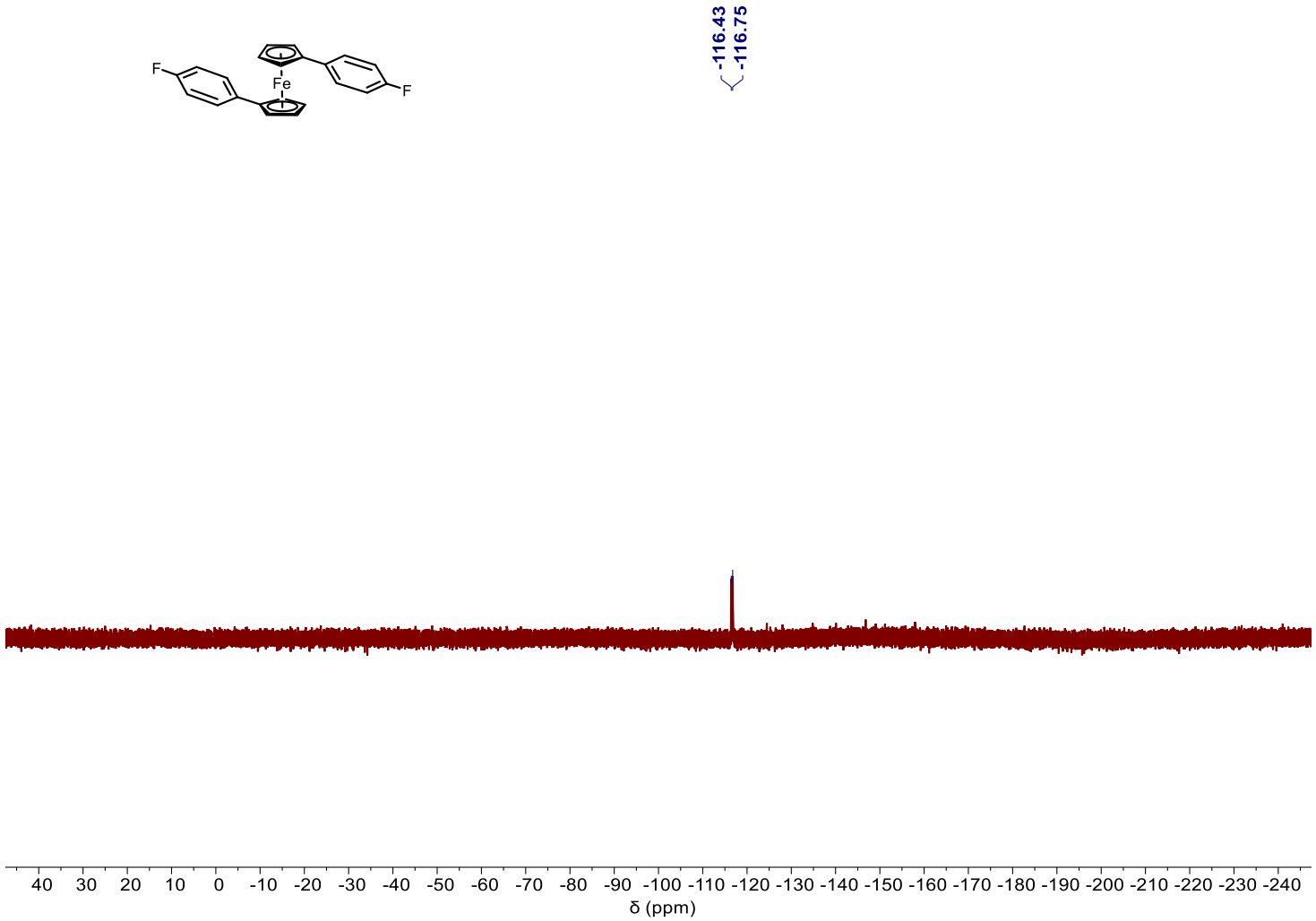


**Figure S21.** $^{19}$F NMR spectrum of **1,1'-FcF** ($CDCl_3$, 565 MHz)

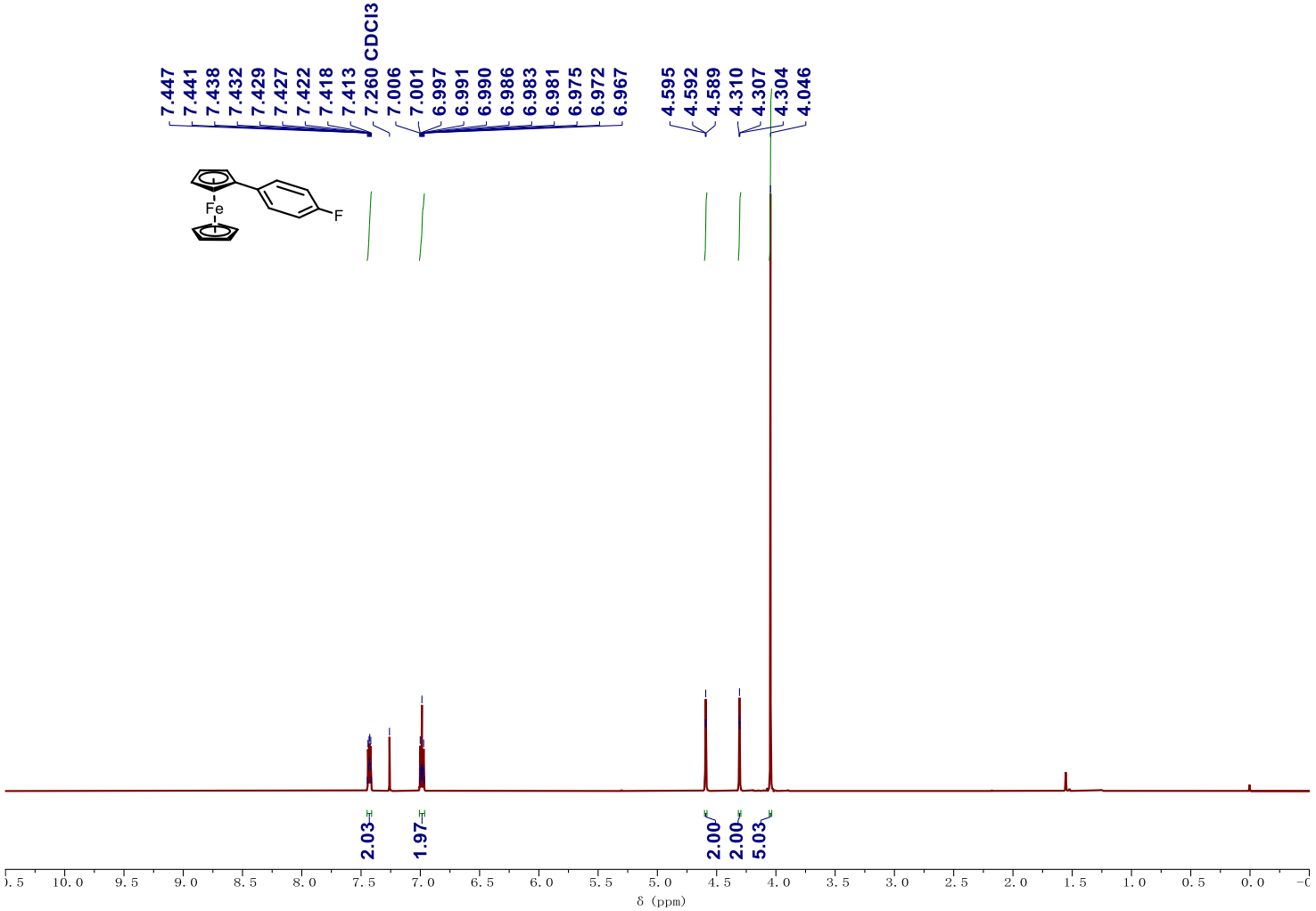


**Figure S22.** $^{1}$H NMR spectrum of **1-FcF** ($CDCl_3$, 600 MHz)

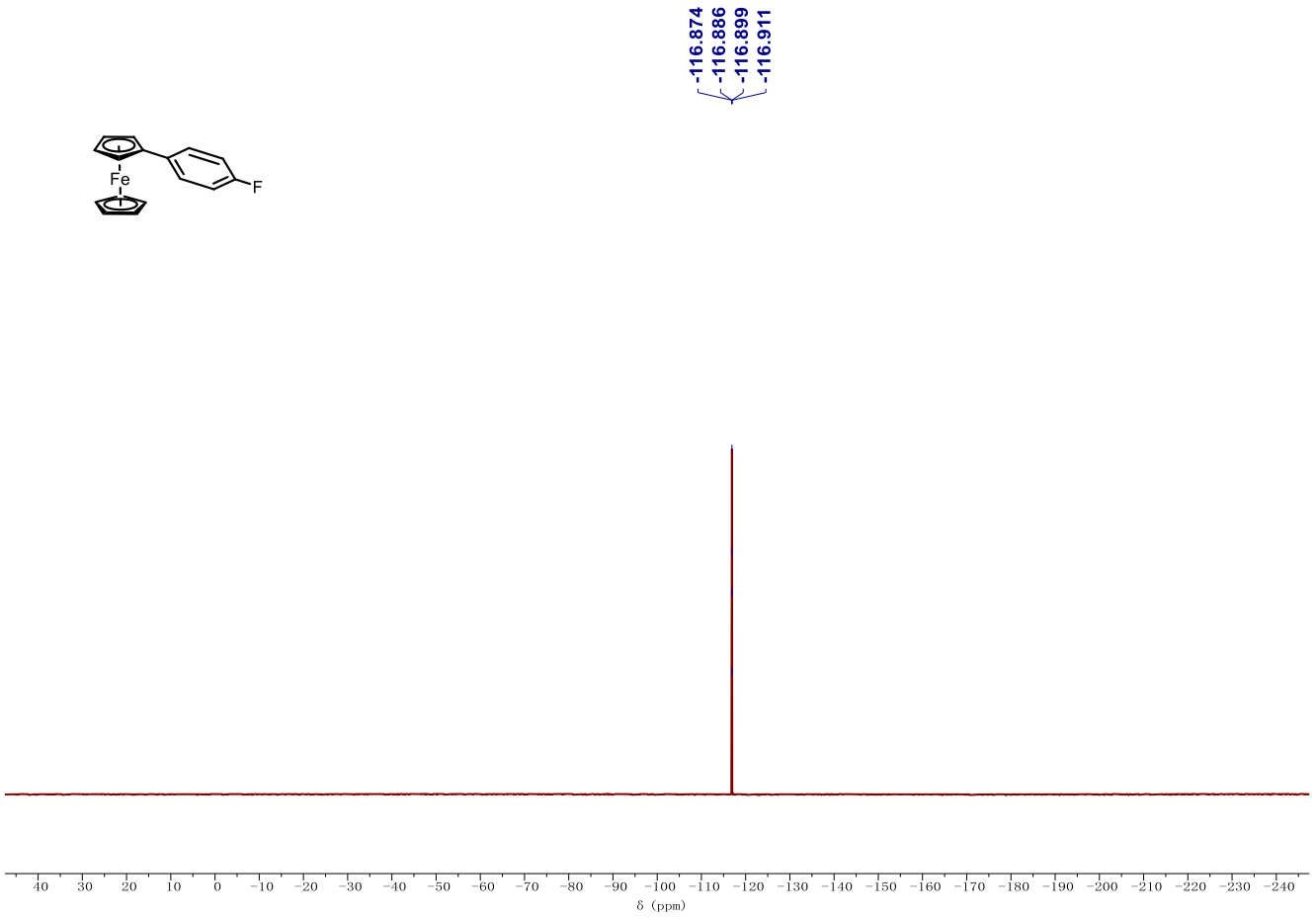


**Figure S23.** $^{19}F$ NMR spectrum of **1-FcF** ($CDCl_3$, 565 MHz)

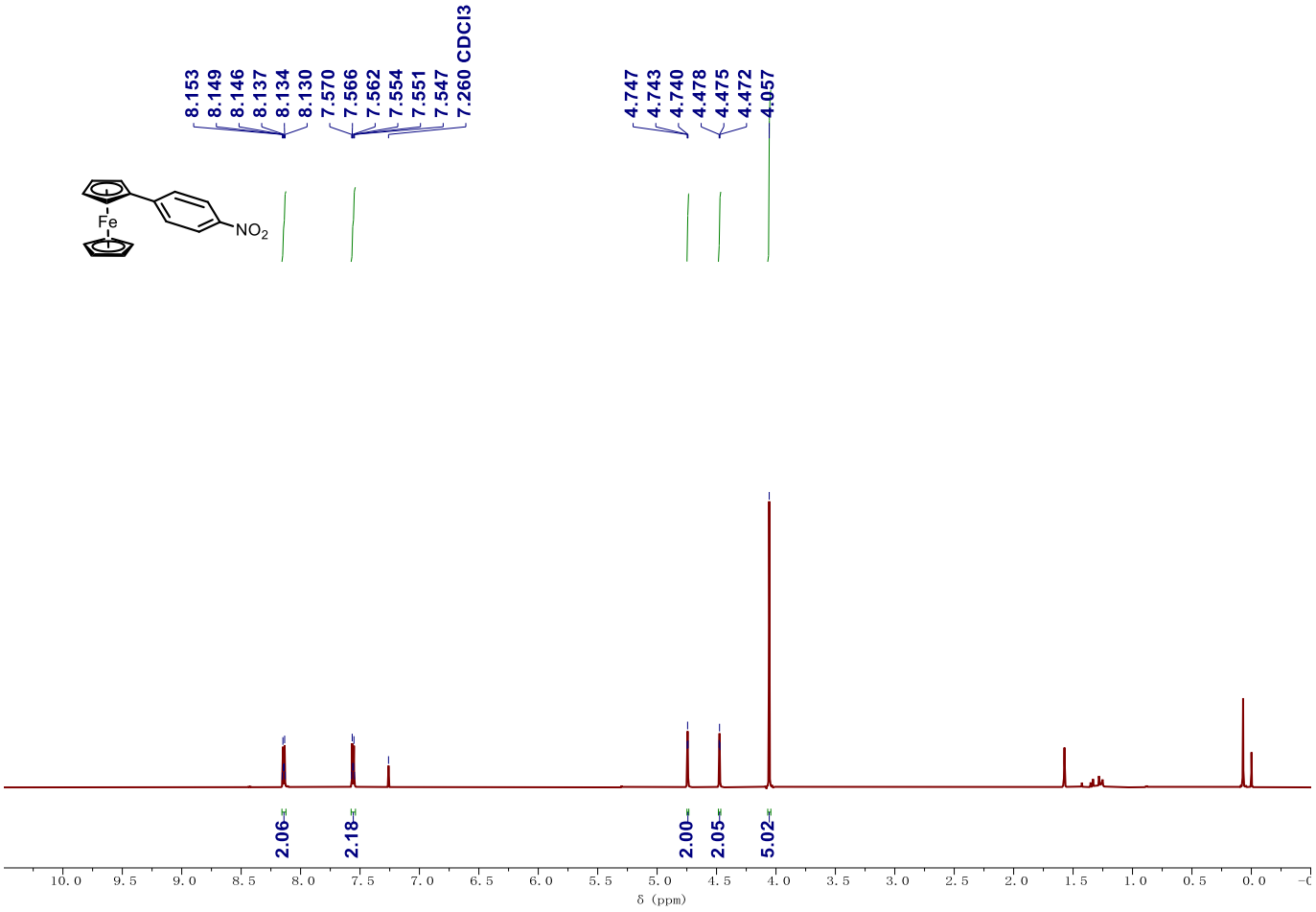


**Figure S24.** $^{1}$H NMR spectrum of **1-FcNO$_2$** ($CDCl_3$, 600 MHz)

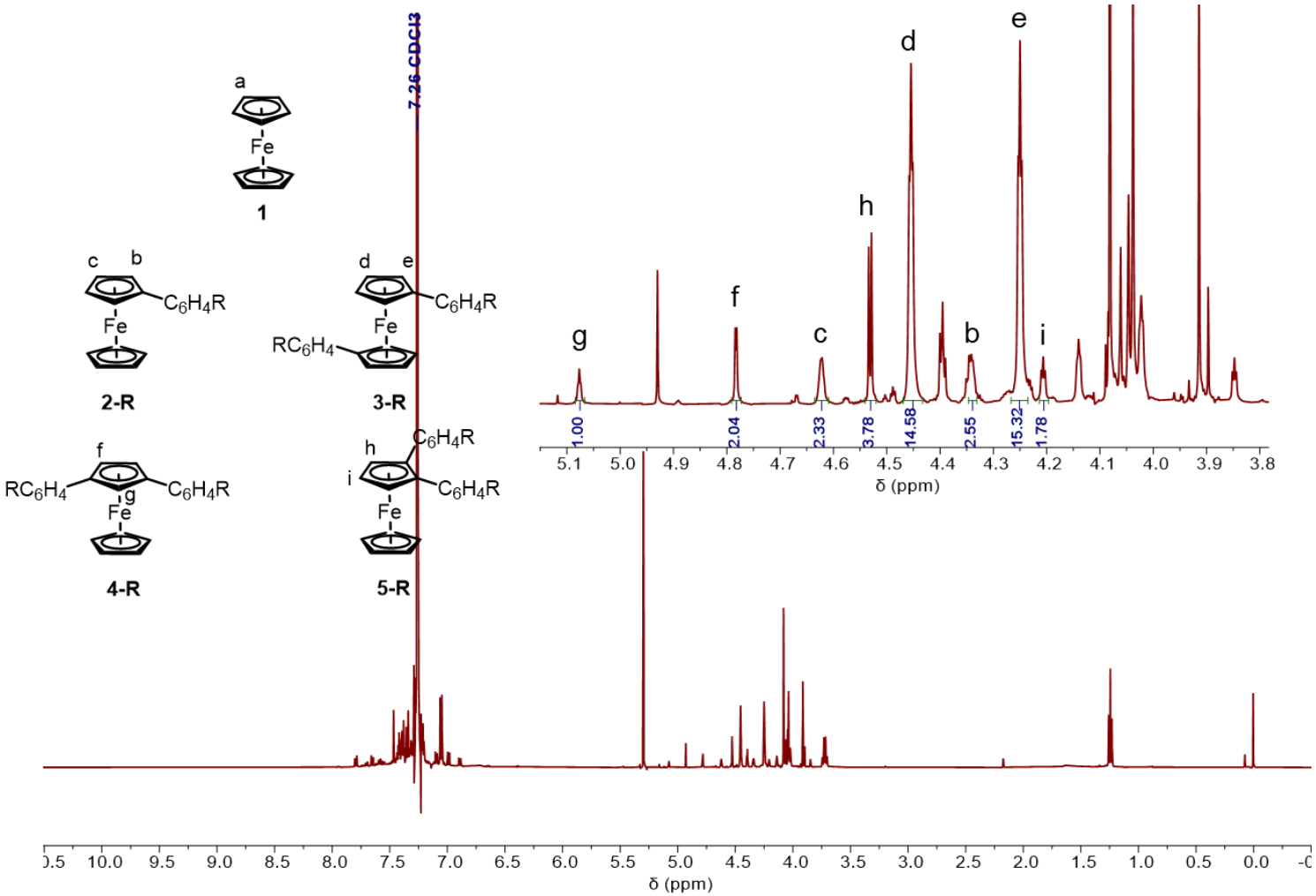


**Figure S25.** $^{1}$H NMR spectrum of the crude reaction mixture of **substrate 1 (R = Br)** ($CDCl_3$, 600 MHz)

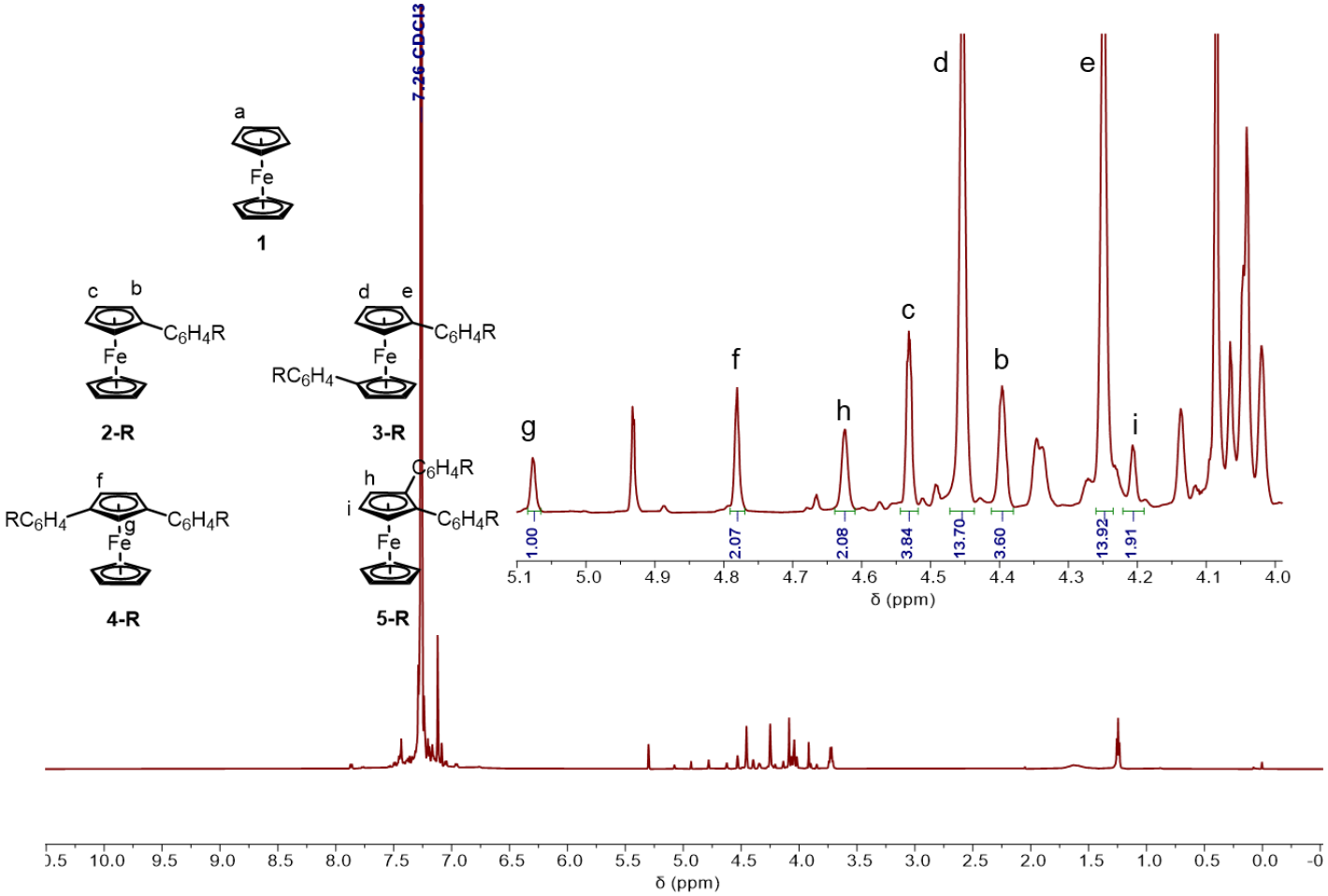


**Figure S26.** $^{1}$H NMR spectrum of the crude reaction mixture of **substrate 1 (R = Cl)** ($CDCl_3$, 600 MHz)

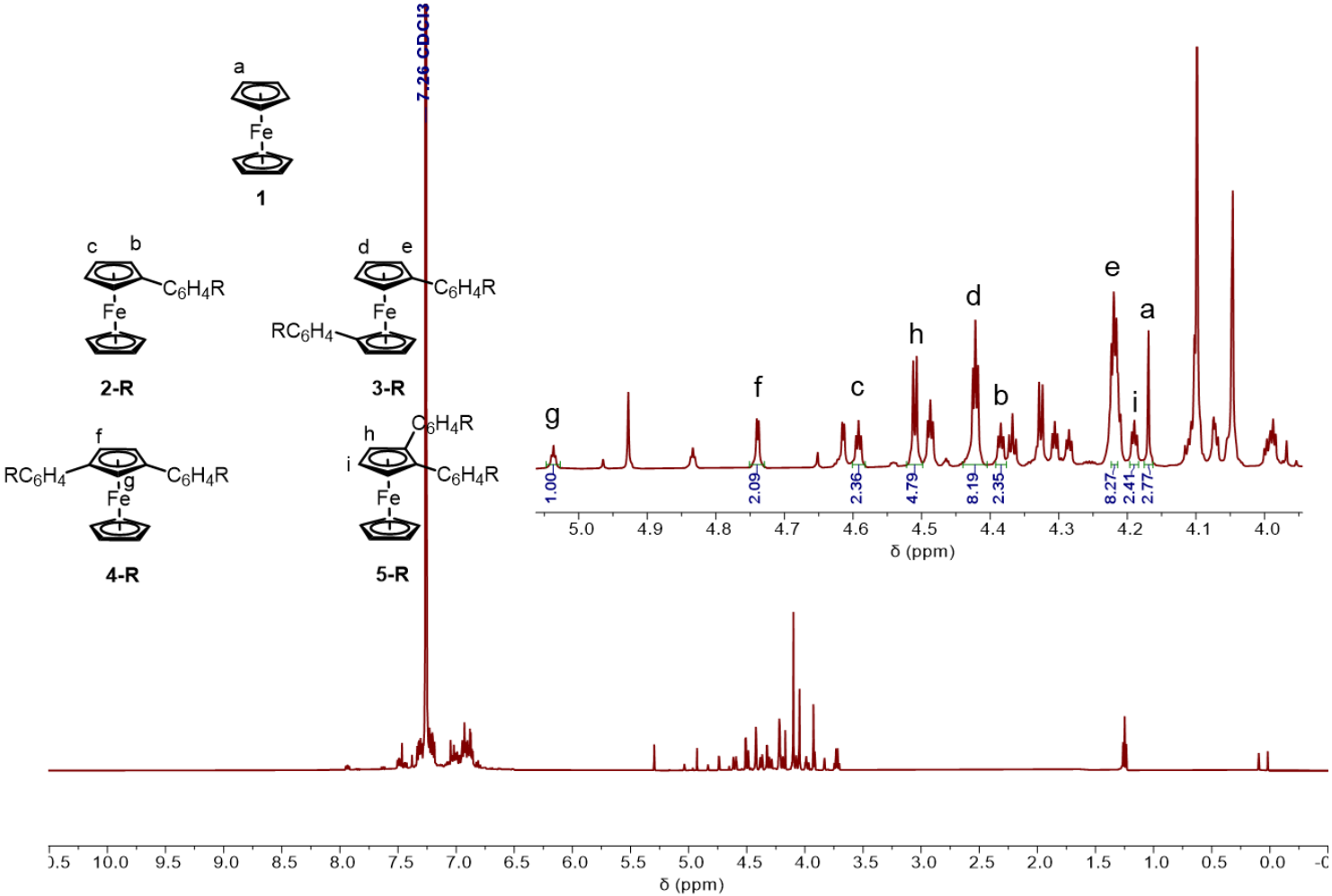


**Figure S27.** $^{1}$H NMR spectrum of the crude reaction mixture of **substrate 1 (R = F)** ($CDCl_3$, 600 MHz)

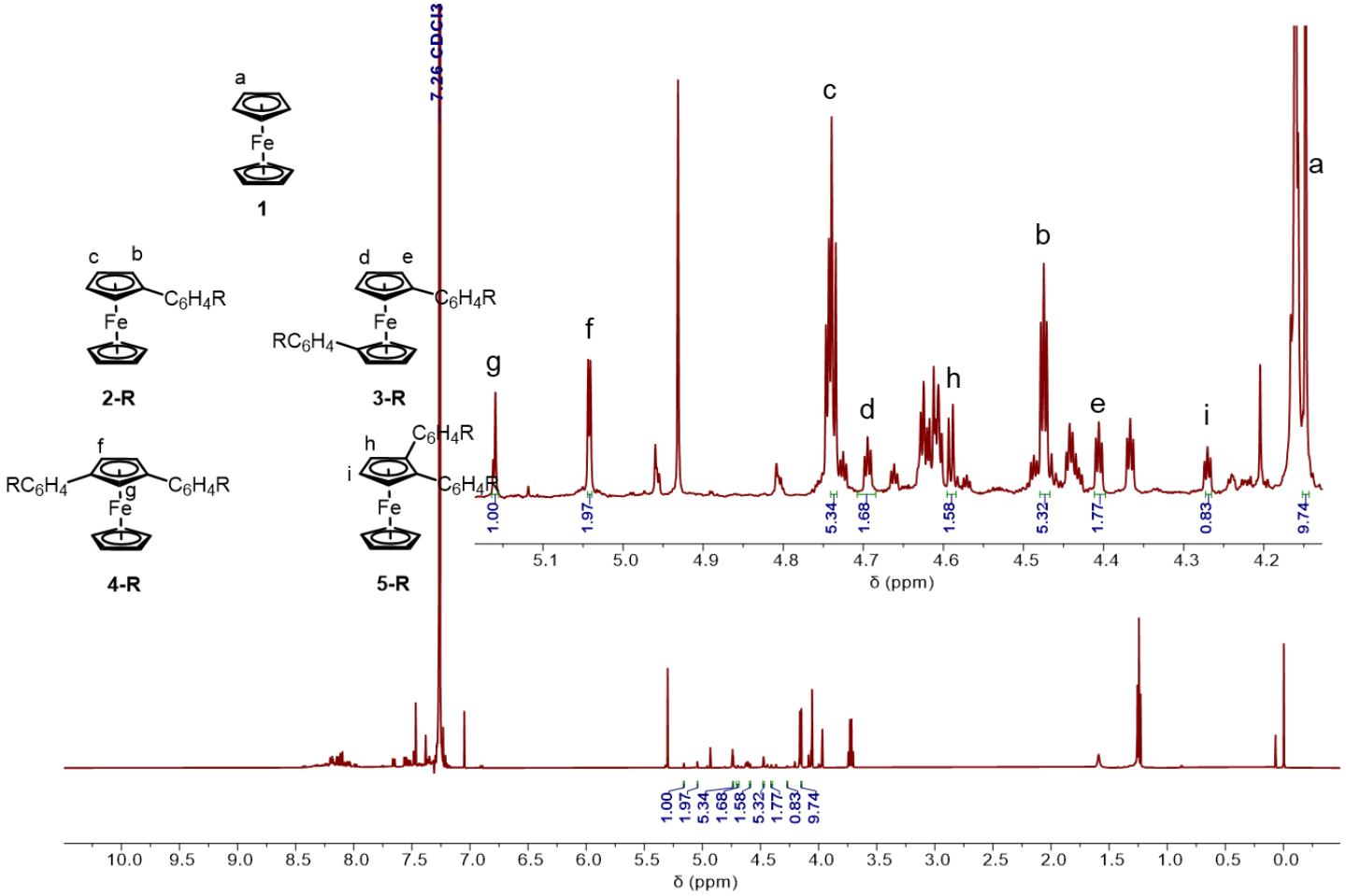


**Figure S28.** $^{1}$H NMR spectrum of the crude reaction mixture of **substrate 1 (R = $NO_2$)** ($CDCl_3$, 600 MHz)

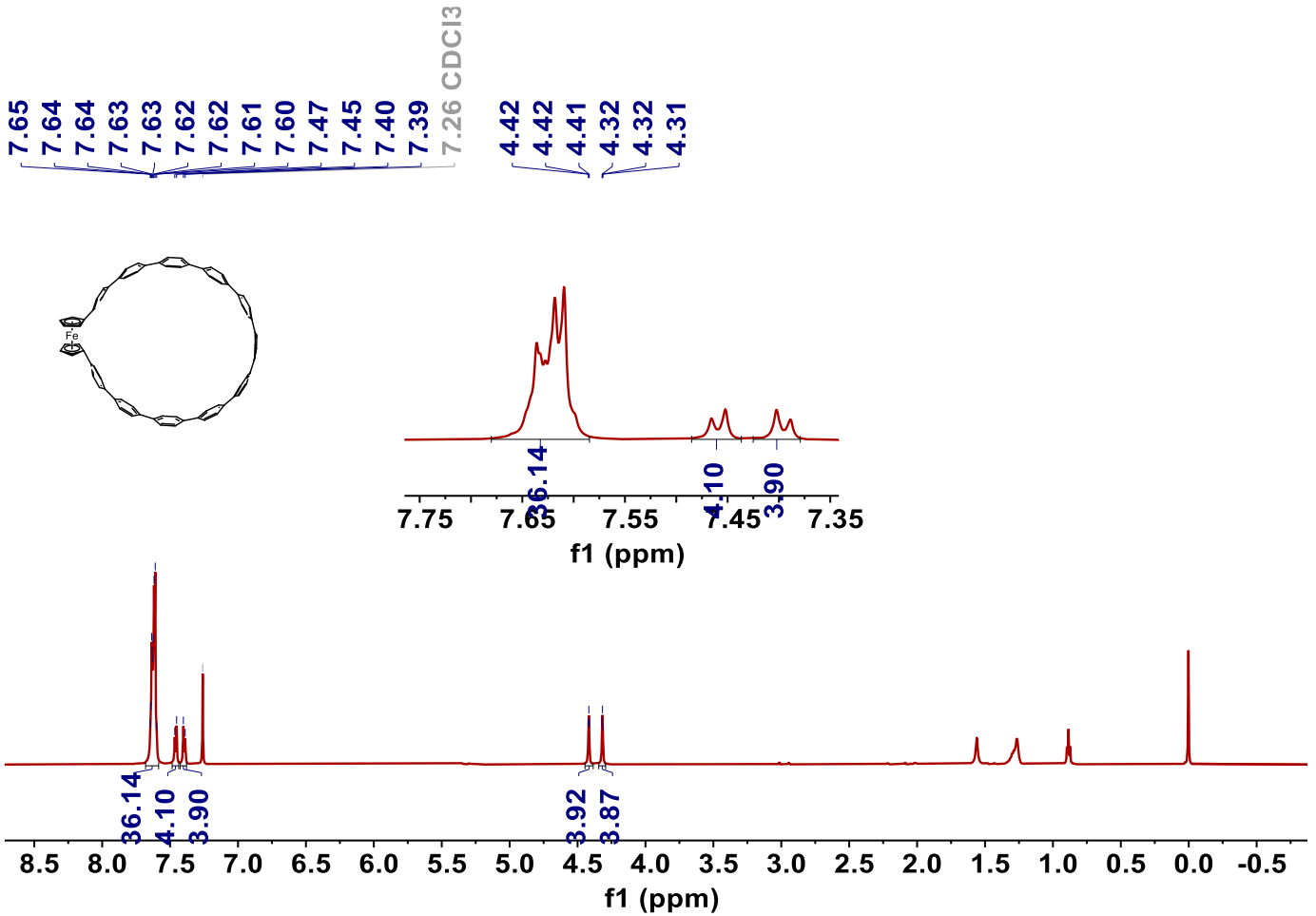


**Figure S29.** $^{1}$H NMR spectrum of **main-Fc[11]CPP** ($CDCl_3$, 600 MHz)

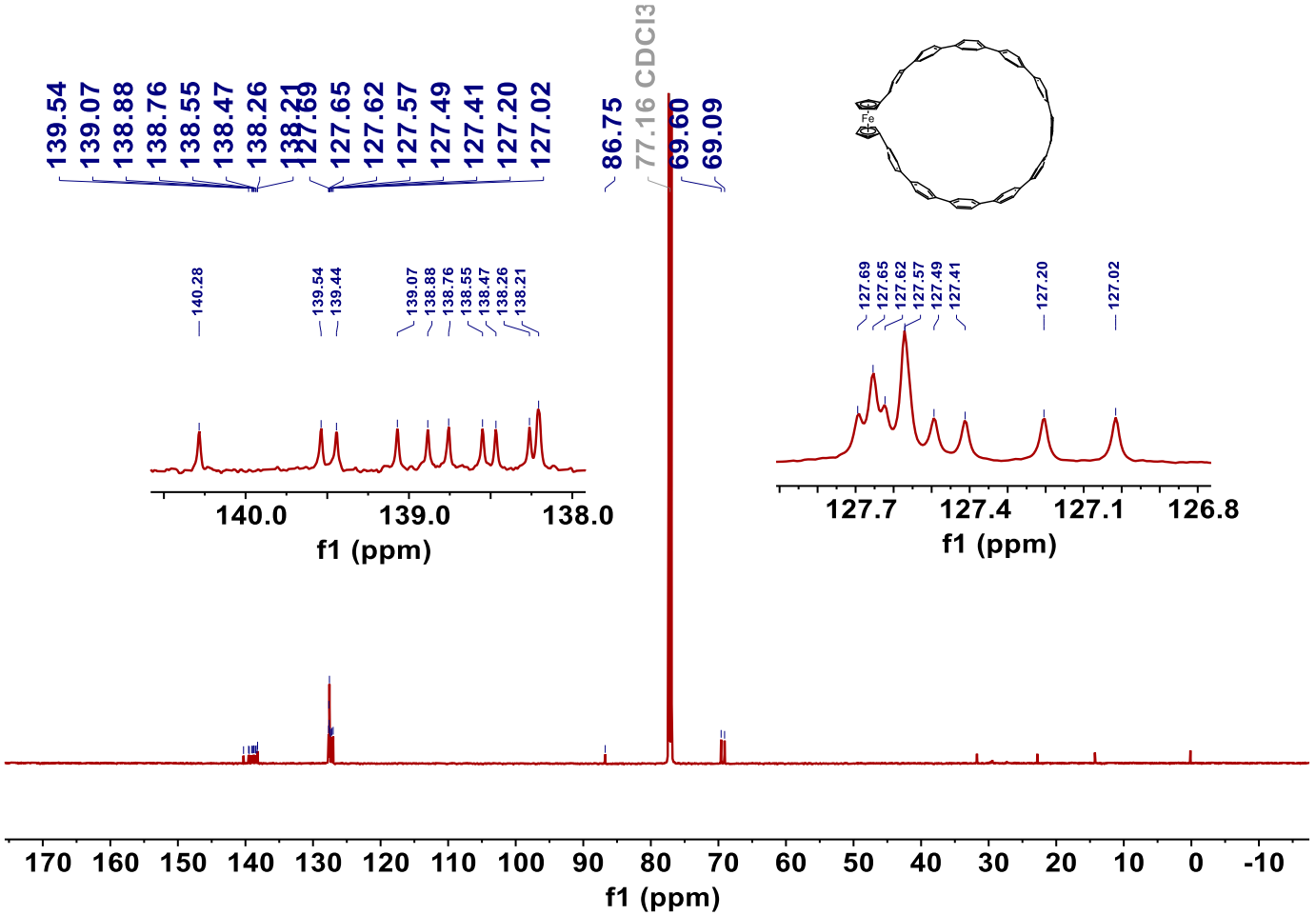


**Figure S30.** $^{13}C$ NMR spectrum of **main-Fc[11]CPP** ($CDCl_3$, 151 MHz)

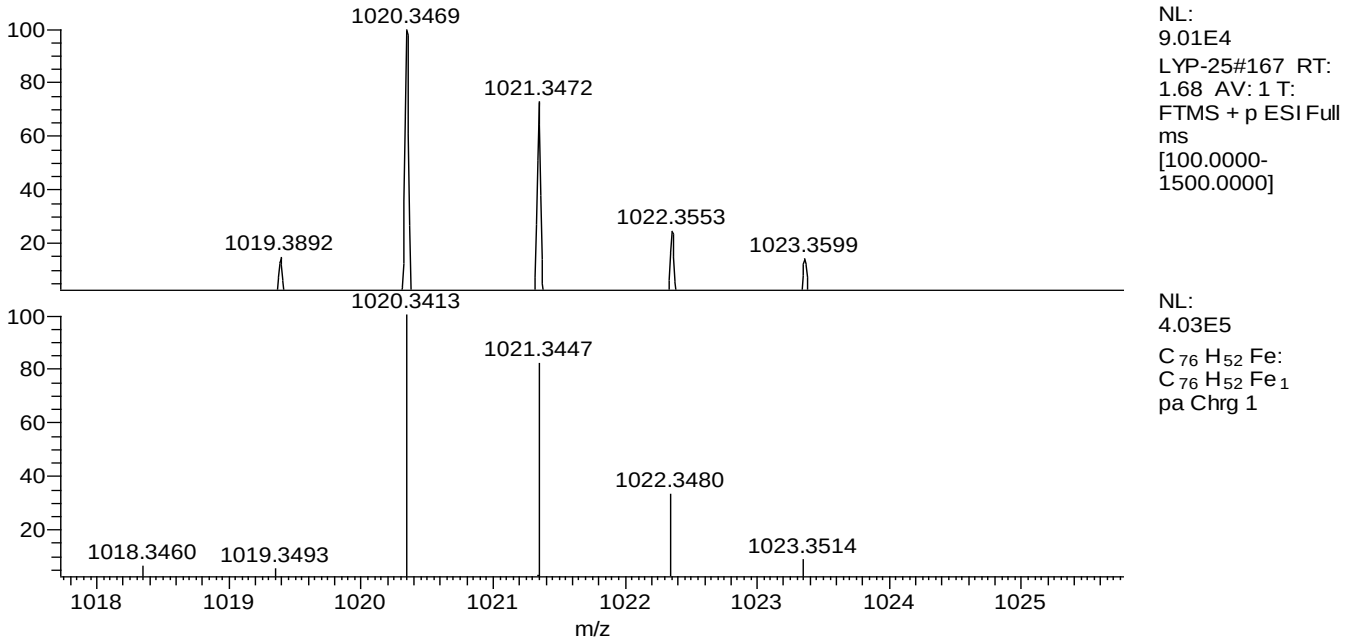


**Figure S31**. HRMS of compound main-Fc[11]CPP (top, the measured; down, Simulated with C76H52Fe)

## 14. Reference


1. CrysAlisPro 2012; Version 1.171.36.31: Agilent Technologies.
2. O. V. Dolomanov, L. J. Bourhis, R. J. Gildea, J. A. K. Howard and H. Puschmann, J Appl Crystallogr. **2009**, *42*, 339-341.
3. G. Sheldrick, Acta Crystallogr. **2015**, *71*, 3-8.
4. Y. Okada and T. Hayashi, Magn Reson Chem. **2005**, *30*, 892-897.
5. H. Yamagishi, T. Fukino, D. Hashizume, T. Mori, Y. Inoue, T. Hikima, M. Takata and T. Aida, J. Am. Chem. Soc. **2015**, *137*, 7628-7631.
6. P. Purushothaman, D. Mohanapriya, K. Thenmozhi and S. Karpagam, New J. Chem. **2024**, *48*, 6893-6901.
7. I. Baumgardt and H. Butenschön, Eur. J. Org. Chem. **2010**, *2010*, 1076-1087.
8. W. Sun, C.-M. Au, K.-W. Wong, K. L. Chan, C. K. Ngai, H. K. Lee, Z. Lin and W.-Y. Yu, ACS Catalysis. **2023**, *13*, 11389-11398.
9. K. Ochiai and S. Fujii, Bioorg Med Chem Lett. **2021**, *46*, 128141.
10. M. Rosenblum, W. G. Howells, A. K. Banerjee and C. W. Bennett, J. Am. Chem. Soc. **1962**, *84*, 2726-2732.
11. J. Xu, B. Lan, L. Zhu, H. Xu, X. Chen, W. Li, Y. Yuan, J. Yan, Y. Li, *Chem. Res. Chinese. U.* **2024**, *40*, 881-886.
12. L. Zhu , J. Xu , B. Lan , X. Chen , H. Kono , H. Xu , J. Yan , W. Li , A. Yagi , Y. Yuan , K. Itami and Y. Li, Org. Chem. Front. **2024**, *11*, 5130-5137.
13. R. C. Gaussian 16 , G. W. T. M. J. Frisch, H. B. Schlegel, G. E. Scuseria, J. R. C. M. A. Robb, G. Scalmani, V. Barone, H. N. G. A. Petersson, X. Li, M. Caricato, A. V. Marenich, B. G. J. J. Bloino, R. Gomperts, B. Mennucci, H. P. Hratchian, A. F. I. J. V. Ortiz, J. L. Sonnenberg, D. Williams-Young, , F. L. F. Ding, F. Egidi, J. Goings, B. Peng, A. Petrone, D. R. T. Henderson, V. G. Zakrzewski, J. Gao, N. Rega, W. L. G. Zheng, M. Hada, M. Ehara, K. Toyota, R. Fukuda, M. I. J. Hasegawa, T. Nakajima, Y. Honda, O. Kitao, H. Nakai, K. T. T. Vreven, J. A. Montgomery, Jr., J. E. Peralta, M. J. B. F. Ogliaro, J. J. Heyd, E. N. Brothers, K. N. Kudin, T. A. K. V. N. Staroverov, R. Kobayashi, J. Normand, A. P. R. K. Raghavachari, J. C. Burant, S. S. Iyengar, M. C. J. Tomasi, J. M. Millam, M. Klene, C. Adamo, R. Cammi, R. L. M. J. W. Ochterski, K. Morokuma, O. Farkas, and a. D. J. F. J. B. Foresman, Gaussian, Inc., Wallingford CT, 2019.
14. T. Lu and F. Chen, J. Comput. Chem. **2012**, *33*, 580-592.
15. W. Humphrey, A. Dalke and K. Schulten, J. Mol. Graphics. **1996**, *14*, 33-38.